Malaria parasite resistance to azithromycin is not readily transmitted by mosquitoes

Hayley D. Buchanan[1,2], Robyn McConville[2,3], Lee M. Yeoh[4,5], Michael F. Duffy[4,5], Justin A. Boddey[2,3], Geoffrey I. McFadden[1] & Christopher D. Goodman[1].

1. School of BioSciences, University of Melbourne, Parkville, 3010, Vic, Australia
2. Walter and Eliza Hall Institute of Medical Research, Parkville, 3052, Vic, Australia
3. Department of Medical Biology, University of Melbourne, Parkville, 3010, Vic, Australia
4. Bio21 Institute, Parkville, 3052, Vic, Australia
5. Department of Microbiology and Immunology, School of Biomedical Sciences, University of Melbourne, Parkville, 3010, Vic, Australia

ABSTRACT

Drug resistance in malaria parasites severely erodes our ability to control disease. Combination therapies—where multiple compounds are combined to reduce the probability of resistance emerging to two or more compounds simultaneously—are the favoured solution to stemming antimalarial resistance. Thus, identifying suitable partner compounds for combinations is a priority. We sought potential partner compounds with inherent refractoriness to the spread of resistance that might better protect the primary antimalarial. We focused on azithromycin, a cheap, safe antibacterial that kills malaria parasites by blocking protein synthesis in the apicoplast—a relict plastid in malaria parasites. Selection for azithromycin resistance in rodent (*Plasmodium berghei*) and human (*P. falciparum*) malaria parasites yielded various mutations in the apicoplast-encoded gene for the 50S large ribosomal subunit protein L4 (Rpl4). *P. berghei* Rpl4 mutant parasites developed poorly in mosquitoes, producing aberrant oocysts and low numbers of sporozoites. *P. falciparum* Rpl4 mutants developed normally in mosquitoes. The azithromycin resistant mutants of both *P. berghei* and *P. falciparum* parasites could establish liver stage infections, but both species developed aberrantly, and *P. berghei* failed to progress to blood stage infections without massive mechanical intervention. The mutations in the apicoplast-encoded ribosomal protein Rpl4 apparently confer azithromycin resistance in the vertebrate blood phase, but the mutations confer a fitness deficit—likely reduced efficiency of apicoplast protein synthesis—that becomes a severe problem for the parasites in the highly-replicative mosquito stage (for *P. berghei*) and liver stage (for both *P. berghei* and *P. falciparum*). The apicoplast is more active metabolically in mosquito and liver stages than blood stage, and we hypothesise that the mutations in apicoplast Rpl4 render it less able to deliver on these metabolic needs, thus retarding parasite development. Azithromycin resistance will therefore be less likely to spread geographically, making it an attractive option as a perennial partner compound to protect appropriate frontline antimalarials from resistance spread.

INTRODUCTION

Drug resistance is a major challenge to controlling, let alone eradicating, malaria (White, 2016). Resistant parasites emerge, spread geographically and eventually erode drug efficacy, often rendering a compound globally useless. We have been in a Sisyphean cycle of using-then-losing malaria drugs for decades (Hyde, 2005). This futile treadmill has repeated itself at least four times, starting in the 1950s with chloroquine and currently playing out with artemisinin, resistance to which has now spread through the Greater Mekong Delta (Ashley et al., 2014; Balikagala et al., 2021; Das et al., 2018; Dondorp et al., 2011; Imwong et al., 2017) and emerged in Africa (Balikagala et al., 2021; Conrad et al., 2023; Fola et al., 2023). Clearly, we need to do things differently. We need to gain more control of malaria drug resistance and stop relying on one promising new drug to replace the previous one that we have set up for failure.

Combination therapies have slowed the spread of artemisinin resistance, and it is likely that any new frontline drug will require protection by some form of partner compound(s). Triple and even quadruple combinations are now being considered (Koehne et al., 2021; van der Pluijm et al., 2021), but to where do we turn for the partner drugs? Older, inexpensive drugs with acceptable safety profiles are one option, but resistance is already circulating for many, which raises the spectre of selecting for multi-drug resistance (Ménard & Fidock, 2019). Ideally, the partner compounds should not only be safe, cheap, compatible, and effective but also be refractory to the spread of resistance, thus prolonging the life of the frontline compound whilst also minimising the risk of selecting for multidrug resistance.

Atovaquone is an antimalarial refractory to the spread of resistance (Balta et al., 2023; Goodman et al., 2016). Atovaquone resistance is unable to be transmitted because resistant parasites with mutations in the mitochondrially-encoded cytochrome *b* suffer fitness deficits during the mosquito phase of their life cycle where they rely on higher rates of mitochondrial electron transport (Goodman et al., 2017; Goodman et al., 2016). In search of further resistance-refractory drugs, we turned to other drug/target systems with similar life cycle constraints. We hypothesised that changes to the parasite fitness landscape when switching from vertebrate to mosquito hosts might also occur in other metabolisms, namely metabolisms that are more active in the insect and/or liver phases of the life cycle than they are in the vertebrate blood stage. An obvious candidate is the apicoplast, a relict plastid of malaria parasites that is substantially more active in mosquito and liver stages (Biddau et al., 2021; Charan et al., 2017; van Schaijk et al., 2014) and for which a wide selection of safe, cheap inhibitors is known (Dahl & Rosenthal, 2007; Goodman et al., 2007; Uddin et al., 2018).

The apicoplast is a non-photosynthetic plastid homologous to the chloroplasts of plants and algae (Köhler et al., 1997; McFadden et al., 1996; McFadden & Yeh, 2017). Apicoplasts have their own DNA and express proteins encoded by their genome using housekeeping machinery within the organelle (Wilson et al., 1996). Apicoplasts, like their chloroplast relatives, arose by endosymbiosis of a photosynthetic cyanobacterium (van Dooren & Striepen, 2013), so their housekeeping machinery (DNA replication, RNA transcription, and protein translation and modification) is bacterial in nature and sensitive to a raft of antibacterials (Botté et al., 2012). For this reason, various antibacterials are also parasiticidal (Botté et al., 2012; Dahl & Rosenthal, 2007;

Dahl & Rosenthal, 2008; Goodman & McFadden, 2013; Goodman et al., 2007). For example, doxycycline, which targets the apicoplast small ribosomal subunit (Chaubey et al., 2005; Dahl & Rosenthal, 2007; Dahl & Rosenthal, 2008), is widely used as a malaria prophylactic (Centers for Disease Control and Prevention, 2013; Rosenthal, 2016) and occasionally for treatment of uncomplicated malaria in conjunction with quinine (Koehne et al., 2021). Similarly, azithromycin is antimalarial (Chandra et al., 2015; Sagara et al., 2014; van Eijk & Terlouw, 2011).

Most drugs targeting apicoplast housekeeping, however, have a key drawback as therapeutics—a delayed onset of parasite death (Dahl & Rosenthal, 2007; Dahl & Rosenthal, 2008; Uddin et al., 2018). The mystery of so-called 'delayed death', where parasite death occurs in the second intraerythrocytic developmental cycle following treatment, was recently solved. Drugged apicoplasts suffer metabolic fatigue that prevents parasite feeding during blood stage, resulting in slow starvation (Kennedy et al., 2019). The slow effect of drugs inhibiting apicoplast housekeeping makes them less useful for treatment, and their use has been relegated to either prophylaxis (Rosenthal, 2016) or—importantly for this study—in combinations with faster acting partners (Centers for Disease Control and Prevention, 2013; Chandra et al., 2015; Dahl & Rosenthal, 2008; Griffith et al., 2007; Lell & Kremsner, 2002; Rosenthal, 2016; van Eijk & Terlouw, 2011). Here, we explore how well resistance to the apicoplast-targeting drug azithromycin is transmitted from vertebrate-to-vertebrate via mosquitoes as a way of assessing whether azithromycin resistance is refractory to geographic spread and thus a potentially useful partner compound.

Azithromycin is a broad-spectrum macrolide antibiotic that blocks apicoplast translation by binding to the peptide exit tunnel of the 50S subunit of the apicoplast ribosome (Sidhu et al., 2007). Azithromycin is used as monotherapy to treat uncomplicated malaria and sometimes in combination with chloroquine or artesunate (Chandra et al., 2015; Sagara et al., 2014; van Eijk & Terlouw, 2011). There are calls to resurrect azithromycin as an antimalarial for combinations (Rosenthal, 2016). This push is strengthened by the recent discovery that azithromycin has two targets in malaria parasites: one in the apicoplast, and a second that inhibits parasite invasion of the red blood cell (Burns et al., 2020; Wilson et al., 2015). Azithromycin is safe for infants and pregnant women and has a very long half-life in the body, all of which make it attractive as a partner compound (Rosenthal, 2016).

Azithromycin is a classic delayed death drug; it is ~100 fold more lethal to malaria parasites during the second red blood cell cycle compared to its effect in the first cycle (Uddin et al., 2018). The apicoplast is the primary target of azithromycin (Sidhu et al., 2007; Uddin et al., 2018). Known resistance mechanisms involve mutations in apicoplast-encoded housekeeping genes (Goodman & McFadden, 2013; Sidhu et al., 2007; Wilson et al., 2015). However, the impact of these apicoplast mutations conferring azithromycin resistance on parasite fitness across the life cycle is unknown.

Investigations into the role of the apicoplast in malaria parasites across the two-host life cycle show that the organelle is essential at every stage (McFadden & Yeh, 2017), but the roles of the apicoplast wax and wane across the life cycle (Buchanan et al., 2022). For instance, in the blood stage the apicoplast has only two roles: to manufacture the five-carbon isoprenoid precursor isopentenyl diphosphate (Uddin et al., 2018; Yeh & DeRisi, 2011), and to synthesise coenzyme A

130 (CoA) (Swift et al., 2021). By contrast, in the mosquito oocyst stage the apicoplast also has to
131 make fatty acids (van Schaijk et al., 2014) and heme (Ke et al., 2014; Nagaraj et al., 2013;
132 Rathnapala et al., 2017), although these metabolic requirements are also species-specific
133 (Buchanan et al., 2022). The apicoplast thus has different roles—and hence demands—in the two
134 hosts, which implies that selection constraints on apicoplast efficiency will differ across the life
135 cycle, much as they do with mitochondrial electron transport (Goodman et al., 2017; Goodman et
136 al., 2016; Jacot & MacPherson, 2016).
137
138 We hypothesised that malaria parasites resistant to azithromycin will experience differential
139 selection across the parasite life cycle and incur a deferred fitness cost that restricts their ability to
140 develop in mosquitoes and in liver stages. In other words, we predicted that apicoplast mutations
141 allowing parasites to survive under drug pressure in the blood stage would be sub-optimal in
142 mosquito and/or liver stages, when drug pressure is released. To test our hypothesis, we generated
143 azithromycin resistant rodent (*Plasmodium berghei*) and human (*P. falciparum*) malaria parasites
144 and assayed their ability to transmit from vertebrate-to-vertebrate via mosquitoes.
145

RESULTS & DISCUSSION

Generation of resistance to azithromycin in vivo in P. berghei and in vitro in P. falciparum

Azithromycin resistance has previously been reported in malaria parasites, but to facilitiate assays of resistance transmissibility, we needed to generate resistance in backgrounds able to be assayed for laboratory transmission. We opted for laboratory generation of azithromycin resistance by serial passage under drug pressure (*in vivo* for *P. berghei* and *in vitro* for *P. falciparum*). Following several months of treatment→recrudescence→treatment cycles with the ED_{95} (60 mg/kg q.d.; Figure 1A and B, Figure S1) and ED_{99} (70 mg/kg q.d.; Figure 1A and B, Figure S1) doses of azithromycin, we obtained three, independently derived lines of *P. berghei* azithromycin resistant parasites. Resistant lines were cloned by limiting dilution and termed PbAZMR_G95D_1, PbAZMR_G95D_2 (selected on a 70 mg/kg q.d. drug regimen), and PbAZMR_S89L (selected on a 60 mg/kg q.d. drug regimen). Since *P. berghei* cannot be cultured *in vitro* for longer than one intraerythrocytic developmental cycle (24-hours), and azithromycin is a delayed-death antimalarial, it was necessary to confirm resistance *in vivo* rather than *in vitro*. Animal ethics constraints limiting the amount of azithromycin administered to mice obviated ED_{50} determinations. Instead, we established the stable resistance of PbAZMR_G95D_1 and PbAZMR_G95D_2 by performing an *in vivo* drug assay using up to twice the ED_{99} dose (140 mg/kg q.d.) of azithromycin (Figure 1C). Both PbAZMR_G95D_1 and PbAZMR_G95D_2 were able to grow consistently in the presence of twice the ED_{99} dose of azithromycin (Figure 1C). The slow growth rate of PbAZMR_S89L (Figure S2) prevented *in vivo* confirmation of resistance, with multiple attempts to obtain high enough blood stage parasitemia failing. We therefore concentrated our efforts on PbAZMR_G95D_1 and PbAZMR_G95D_2.

We selected for azithromycin resistance *in vitro* in the *P. falciparum* mosquito-transmissible strain NF54. The IC_{50} of azithromycin in a 120-hour delayed-death assay was 0.059 ± 0.017 μM (Figure 1D and E). Two independent cultures of a clonal line of NF54, and one of a clonal line of the non-transmissible 3D7 strain, were grown in the presence of 300 nM azithromycin for 96-hours and then maintained in drug-free culture for 24 days, at which time parasites recrudesced and grew normally in 300nM azithromycin. Time to recrudescence for azithromycin was similar (24-32 days) for parasites selected for resistance with pyrimethamine or atovaquone. The azithromycin resistant parasites continued to grow normally whe drug was increased to 600 nM (Figure 1D). All three mixed lines showed azithromycin IC_{50}s ~100 fold greater than the parental line, and this level of resistance was maintained in all lines following cloning, with Pf_AZMR_C4 and Pf_AZMR_D2 exhibiting IC_{50}s of 5.63 ± 0.87 μM and 5.29 ± 0.53 μM respectively (Figure 1D and E).

Azithromycin resistance in P. berghei and P. falciparum is apparently conferred by mutations in Rpl4.

It is well established that azithromycin targets apicoplast translation in malaria parasites, specifically the 50S ribosomal subunit (Dahl & Rosenthal, 2007; Sidhu et al., 2007). Moreover, reported resistance to azithromycin in malaria parasites is conferred by apicoplast-encoded mutations (Goodman et al., 2013; Sidhu et al., 2007; Wilson et al., 2015). Whole genome sequencing of several clones of each of our independently generated *P. berghei* and *P. falciparum* azithromycin resistant lines revealed mutations in a conserved region of the apicoplast-encoded 50S ribosomal protein L4 (Rpl4; PBANKA_API00430 in *P. berghei* and PF3D7_API01300 in *P.*

191 *falciparum* respectively; Figure 1F). Two different point mutations in Rpl4, S89L and G95D, were
192 found in *P. berghei* (Figure 1F). Another mutation, G76V, was found in Rpl4 of azithromycin
193 resistant *P. falciparum* (Figure 1F). These Rpl4 point mutations were observed in the absence of
194 any other identifiably relevant point mutations, indels, or copy number variations.
195
196 The mutations in both species reside in a region of Rpl4 that flank the ribosome exit tunnel where
197 macrolides like azithromycin bind (Dao Duc et al., 2019). It is a region of high sequence identity
198 across apicoplasts of other apicomplexan parasites, chloroplasts of plants and algae, and bacteria
199 (Figure 1F). The corresponding Rpl4 G95D mutation seen in our *P. berghei* azithromycin resistant
200 parasites also confers azithromycin resistance in *P. falciparum* (Wilson et al., 2015) and resistance
201 to erythromycin (a closely related macrolide) in chloroplasts of the alga *Chlamydomonas*
202 *reinhardtii* (Bowers et al., 2003). Moreover, the Rpl4 G76V mutation generated here in *P.*
203 *falciparum* has been previously reported to confer azithromycin resistance in *P. falciparum* (Sidhu
204 et al., 2007), as well as in the bacteria causing gonorrhea and pneumococcal disease (Canu et al.,
205 2002; Ma et al., 2020)(Figure 1F). In zoonotic infections of *Babesia microti,* three different Rpl4
206 mutations in the same region are associated with azithromycin resistance (Marcos & Wormser,
207 2023).
208
209 Taken together, the genotyping strongly suggests that the apicoplast-encoded Rpl4 mutations in
210 our *P. berghei* and *P. falciparum* azithromycin resistant parasites confer azithromycin resistance.
211 However, there are no protocols to genetically modify the apicoplast genome, so we cannot
212 reconstitute these mutations to demonstrate unequivocally that these point mutations are sufficient
213 to confer resistance.
214
215 *Azithromycin resistant P. berghei parasites are severely impaired during mosquito stage*
216 *development*
217 To test the sexual viability of our *P. berghei* azithromycin resistant strains we first quantified the
218 numbers of male gametocytes that underwent exflagellation to produce male gametes. No
219 significant difference for number of exflagellations between azithromycin resistant parasites
220 (PbAZMR_G95D_1, PbAZMR_G95D_2, PbAZMR_S89L) and *P. berghei* wildtype (Pb_WT)
221 control was found (Figure 2A). PbAZMR_S89L parasites produced the least number of
222 exflagellating male gametocytes, but poor blood stage growth of this mutant (Figure S2) limited
223 us to only two independent counts, so we cannot say if this reduction is significant.
224
225 We next infected female *Anopheles stephensi* mosquitoes with our azithromycin resistant lines and
226 Pb_WT control parasites by allowing the mosquitoes to bite infected mice. There was no
227 significant difference in the prevalence of mosquito infection between all our azithromycin
228 resistant strains compared to Pb_WT, but again PbAZMR_S89L parasites were the least infective
229 (Figure 2B). Our three *P. berghei* azithromycin resistant strains developed significantly fewer
230 midgut oocysts per mosquito at 9-14 days post blood feed (Figure 2B). Except for PbAZMR_S89L
231 (for reasons discussed above), we performed a minimum of five independent *A. stephensi* mosquito
232 infections with PbAZMR_G95D_1, PbAZMR_G95D_2 and Pb_WT strains and saw means of 114
233 (89 infected midguts counted), 191 (48 infected midguts counted) and 261 (105 infected midguts
234 counted) oocysts per midgut respectively (Figure 2B). The reduction of oocysts in

PbAZMR_G95D_2 infected mosquitoes compared to Pb_WT was less severe than for PbAZMR_G95D_1 (Figure 2B). This may be simple biological variation, but we cannot discount that PbAZMR_G95D_2 has a compensatory mechanism restoring some mosquito infectivity. The severe impairment seen in PbAZMR_S89L parasites during mosquito midgut development is likely linked to the very slow blood stage growth, and thus a lack of sexual stage development, commencing with fewer exflagellations and flowing on to lower infection rates and less oocysts (Figure 2A).

At 20-26 days post blood feed, salivary glands were dissected from mosquitoes infected with our azithromycin resistant strains PbAZMR_G95D_1, PbAZMR_G95D_2, PbAZMR_S89L, and Pb_WT. Again, all our azithromycin resistant lines produced significantly fewer salivary gland sporozoites than Pb_WT (Figure 2C).

To visualise oocyst development in our azithromycin resistant strains, we performed an immunofluorescence assay (IFA) on whole, infected mosquito midguts (Figure 2D). Although IFA of whole midguts is informative, it is not quantitative. The epithelial and basal lamina cells of the *A. stephensi* midgut, as well as the *P. berghei* oocyst wall, present significant barriers to consistent reagent entry and exit. Nevertheless, PbAZMR_G95D_1 oocysts were observed to have dispersed staining with the apicoplast-directed antibody to anti-acyl carrier protein (ACP), whereas Pb_WT oocysts showed the expected branched apicoplast pattern (Figure 2D). ACP is encoded in the parasite nucleus and targeted to the apicoplast (Waller et al., 1998; Waller et al., 2000) and continues to be produced even if the apicoplast is not intact. The dispersed ACP staining seen in our PbAZMR_G95D_1 oocysts suggests that the apicoplast structure has been disrupted, and ACP is likely accumulating in vesicles destined for the non-existent or deformed apicoplast.

The qualitative defects in oocyst apicoplasts of azithromycin resistant *P. berghei* parasites prompted us to quantify apicoplast health in our mutants. We performed quantitative PCR (qPCR) on total genomic DNA isolated from *A. stephensi* midguts infected with either our *P. berghei* azithromycin resistant strains or WT parasites to assess the relative copy numbers of both the mitochondrion and apicoplast genomes based against nuclear genome copy number (Figure 2E). Intriguingly, we saw a drop in the apicoplast genome copy number in all the *P. berghei* azithromycin resistant strains, with a mean percent drop of 74.33%, 76.11% and 82.82% for PbAZMR_G95D_1, PbAZMR_G95D_2, and PbAZMR_S89L respectively (Figure 2E). Of note, there appears to be a concomitant increase in mitochondrial genome copy number in all the azithromycin resistant strains compared to Pb_WT (Figure 2E). We are uncertain whether this is due to a reduction in nuclear DNA, thus affecting the normalisation step for the azithromycin resistant parasites, or potentially related to non-synchronous timing of genome replication of each of the organelles. Nevertheless, the data overall suggests azithromycin resistance-conferring mutations in apicoplast-encoded Rpl4 are causing a disruption to parasite development during mosquito stages in *P. berghei* concomitant with apicoplast malaise.

Azithromycin resistant P. falciparum parasites develop normally in mosquitoes

To determine if azithromycin resistance mutations impeded *P. falciparum* mosquito stage development, we selected a single clone (Pf_AZMR_C4, hereafter Pf_AZMR) to conduct downstream analyses. We performed standard membrane feeding assays with mature stage V gametocytes from Pf_AZMR, and the parent line *P. falciparum* NF54 wildtype (Pf_WT), and compared their development in female *A. stephensi* mosquitoes. Both Pf_AZMR and Pf_WT parasite lines produced equivalent numbers of mature stage V gametocytes (Figure 2F). Similarly, both Pf_AZMR and Pf_WT parasites produced equivalent numbers of midgut oocysts at day 7 post blood feed, with an equivalent infection prevalence (Figure 2G). Furthermore, Pf_AZMR and Pf_WT parasites had no significant difference in the number of salivary gland sporozoites at day 17 post blood feed (Figure 2H). Thus, Pf_AZMR, despite having a point mutation in Rpl4 near those that severely disrupt mosquito infectivity of Rpl4 mutants in *P. berghei*, is apparently uninhibited in its ability to infect mosquitoes.

Azithromycin resistant P. berghei sporozoites lose their apicoplast

To further probe downstream effects of the aberrant apicoplast development in our *P. berghei* azithromycin resistant parasites, we performed an IFA on both the PbAZMR_G95D_1 and PbAZMR_G95D_2 sporozoites to visualise apicoplast morphology (Figure 3A). Surprisingly, both PbAZMR_G95D_1 and PbAZMR_G95D_2 sporozoites appeared to lack any defined apicoplast, only having diffuse ACP staining throughout the length of the sporozoite (Figure 3A), whereas Pb_WT sporozoites have a canonical, distinct, punctate apicoplast structure adjacent the nucleus as expected, in addition to some diffuse staining (Figure 3A). The diffuse apicoplast staining seen in azithromycin resistant sporozoites (Figure 3A) is reminiscent of the dispersed apicoplast marker labelling in oocysts of azithromycin resistant parasites and may indicate some ACP trafficking. To quantify this aberration, we assessed >100 sporozoites from each parasite strain, across three independent mosquito infections (and hence, three separate IFA experiments) (Figure 3B). Only 12.6% of PbAZMR_G95D_1 sporozoites, and 18.8% of PbAZMR_G95D_2 sporozoites exhibited intact apicoplasts, whereas 93% of Pb_WT sporozoites had clearly identifiable, punctate apicoplasts (Figure 3B). Together, these data suggest that Rpl4 mutations conferring azithromycin resistance disrupt apicoplast integrity during *P. berghei* mosquito stage development, culminating in the production of sporozoites that predominantly lack an apicoplast.

To assess potential viability of these azithromycin resistant sporozoites, we performed a sporozoite gliding motility assay comparing the movement of PbAZMR_G95D_1 and PbAZMR_G95D_2 sporozoites to Pb_WT sporozoites (Figure 3C). PbAZMR_G95D_1 and PbAZMR_G95D_2 sporozoites are somewhat impaired in their gliding motility compared to Pb_WT, but the differences were not statistically significant (Figure 3C). Motility of the PbAZMR_G95D_1 and PbAZMR_G95D_2 sporozoites, despite mostly lacking a distinct apicoplast, is congruent with the fact that they had successfully made the journey from the midgut to the mosquito salivary glands (Figure 2B). Previous studies have noted, however, that even a modest reduction in sporozoite gliding can severely impact *in vivo* infectivity of sporozoites (Ejigiri et al., 2012; Hopp et al., 2015). Thus, the motility differences observed here, although not statistically significant, may be biologically relevant to the infectivity of azithromycin resistant sporozoites, particularly *in vivo*.

323 *Azithromycin resistant P. berghei parasites are critically diminished in their capacity to establish*
324 *an infection in a naïve vertebrate host*

325 After assaying the *P. berghei* azithromycin resistant parasites through mosquito stage development
326 and showing that they produce fewer sporozoites—most of which lack a distinct apicoplast—we
327 next tested their ability to establish a patent infection in a naïve vertebrate host, either by bites
328 from infected mosquitoes or direct intravenous (IV) injection of isolated sporozoites. Neither
329 PbAZMR_G95D_1 or PbAZMR_G95D_2 was able to establish a patent infection in naïve mice
330 bitten by at least 15 infected *A. stephensi* mosquitoes (Figure 4A). Similarly, IV injection of $1x10^3$
331 PbAZMR_G95D_1 or PbAZMR_G95D_2 sporozoites failed to produce patent infections (Figure
332 4B), whereas Pb_WT sporozoites reliably produced infections with a time to patency (observed
333 by microscopy of Giemsa stained thin blood smears) of 3-4 days (Figures 4A and B). When the
334 inoculum of IV injected sporozoites was increased to $1x10^4$ sporozoites, PbAZMR_G95D_2
335 sporozoites were able to establish a patent blood stage infection in all of six attempts (Figure 4C).
336 It is important to note though that patency for the resistant mutant required 4-13 days (mean 8.5
337 days ± 3.8 days; Figure 4C), whereas Pb_WT sporozoites produced a patent infection in 3 days for
338 all of 10 attempts (Figure 4C). DNA sequencing confirmed that the G95D Rpl4 mutation was
339 present in the newly established PbAZMR_G95D_2 passage zero (P0) infection (data not shown).
340 PbAZMR_G95D_1 sporozoites were unable to produce a patent infection in a naïve host in five
341 attempts of IV injection of $1x10^4$ sporozoites (Figure 4C). Thus, through substantial mechanical
342 intervention to provide a large sporozoite inoculum directly into a vein, we were able to achieve
343 transmission of PbAZMR_G95D_2 but not PbAZMR_G95D_1. Even then, the
344 PbAZMR_G95D_2 parasites showed a clear fitness defect over and above their liver stage delay,
345 with blood stage parasites failing to increase substantially in parasitaemia when monitored over
346 14 days post sporozoite IV injection (Figure 4D).

347

348 These data again suggest there is a difference in phenotype penetrance between
349 PbAZMR_G95D_1 and PbAZMR_G95D_2, which recapitulates similar differences during
350 mosquito stage development. Despite both resistant mutants having the same azithromycin
351 resistance conferring Rpl4 mutation, there remains a slight fitness advantage in the
352 PbAZMR_G95D_2 parasites over the PbAZMR_G95D_1 parasites. There is, however, still a
353 significant deficiency in the PbAZMR_G95D_2 sporozoites in that they are only transmission-
354 competent when directly IV injected; and then only in massive numbers (Figures 4A-C). The clear
355 difficulty (or block in the case of PbAZMR_G95D_1) in the ability of our *P. berghei* azithromycin
356 resistant parasites to establish a patent infection in a naïve host points to liver stage developmental
357 defects, and the significant delay in patency of P0 infections induced by PbAZMR_G95D_2
358 sporozoites is consistent with this. This is not surprising given the importance of a proper
359 functioning apicoplast during *P. berghei* liver stage development (Falkard et al., 2013; Stanway et
360 al., 2019; Vaughan et al., 2009; Yu et al., 2008). Indeed, while some transmission of
361 PbAZMR_G95D_2 is feasible, the parasites exhibit impaired development during mosquito
362 stages, liver stages, and transmission to naïve hosts, identifying a clear fitness cost associated with
363 the G95D Rpl4 mutation.

364

365 *Late liver stage development of azithromycin resistant P. berghei parasites is impeded*

366 To investigate further the apparently aberrant liver stage development of our *P. berghei*
367 azithromycin resistant strains, we inoculated *in vitro* grown HC-04 hepatocytes with sporozoites

368 and observed the parasites by IFA to measure size and observe the morphology of the apicoplasts
369 and nuclei. Firstly, we wanted to confirm whether PbAZMR_G95D_1 sporozoites are even able
370 to infect liver cells given that they were unable to establish a blood stage infection in a naïve host
371 by any method attempted. Secondly, while PbAZMR_G95D_2 sporozoites are clearly impeded in
372 their ability to establish a blood stage infection in a naïve host, we wanted to examine the reasons
373 for the apparent liver stage developmental delay and requirement for such massive sporozoite
374 numbers to establish an infection in a malaria naïve host at all. Thirdly, we wanted to observe any
375 associated aberrations in apicoplast morphology and development of nuclei during liver stage
376 development of PbAZMR_G95D_1 and PbAZMR_G95D_2.
377
378 Preliminary analyses revealed no differences in liver stage schizont size between azithromycin
379 resistant parasites and Pb_WT at 24-hours post inoculation (data not shown). We therefore
380 concentrated our efforts, and limited sporozoite supply, on a later liver stage timepoint of 48-hours.
381
382 IFA of liver cells inoculated with PbAZMR_G95D_1, PbAZMR_G95D_2 or Pb_WT sporozoites
383 after 48 hours of development revealed marked difference in morphology (Figure 4E). WT liver
384 stage schizonts, irrespective of size, typically showed reticulated ACP staining, indicative of
385 normal apicoplast morphology at this point of liver stage development (Stanway et al., 2009) (top
386 two panels, Figure 4E). Furthermore, the nuclei of Pb_WT liver stage schizonts showed clear
387 differentiation with each nucleus beginning to be associated with a developing merozoite (top two
388 panels, Figure 4E). Contrast this with the PbAZMR_G95D_1 and PbAZMR_G95D_2 liver stage
389 schizonts at 48-hours post infection where the ACP staining marking the apicoplast was cloudy
390 and diffuse (bottom two panels, Figure 4E), reminiscent of what is seen in oocysts and sporozoites
391 with these strains. Additionally, the nuclei of PbAZMR_G95D_1 and PbAZMR_G95D_2
392 developing liver stage schizonts appeared aggregated, forming unusual donut-shaped clusters
393 (bottom two panels, Figure 4E). These images are typical of what we observed for 48-hour liver
394 stages. To quantify these observations, we used maximum projections of 48-hour post infection
395 IFAs over two biological replicates and measured the size of each liver stage schizont, and we also
396 quantified the nuclei in each developing parasite (Figure 4F and 4G). Both PbAZMR_G95D_1
397 (n=31) and PbAZMR_G95D_2 (n=47) liver stage parasites were significantly smaller than WT
398 (n=60; Figure 4F) and contained fewer nuclei (Figure 4G). Moreover, this reduction in nuclei was
399 independent of liver stage parasite size because normalising number-of-nuclei to the area of the
400 liver stage parasite optical section still showed significantly fewer nuclei in PbAZMR_G95D_1
401 and PbAZMR_G95D_2 parasites compared to Pb_WT (Figure 4H). These late liver stage data
402 essentially recapitulate the phenotype seen during development throughout mosquito stages; i.e.
403 aberrant apicoplast morphology, and inability to properly differentiate nuclei. In sum, these defects
404 in apicoplast integrity and nuclei biogenesis at both the oocyst and liver stages of the life cycle
405 appear to severely hamper or even abrogate transmission of our *P. berghei* azithromycin resistant
406 parasites.
407
408 *Phenotypes converge: liver stage development of azithromycin resistant P. falciparum parasites*
409 *is impeded similar to P. berghei*
410 To investigate further the effects of apicoplast-encoded G76V azithromycin resistance mutation
411 on the life cycle progression of *P. falciparum*, we measured the rates of liver cell traversal (3-hours
412 post inoculation) and invasion (18-hours post inoculation) of Pf_AZMR and Pf_WT sporozoites

413 (Figure 5A, 5B). Reflecting the apparently near-normal motility of azithromycin resistant *P.*
414 *berghei* sporozoites, azithromycin resistant Pf_AZMR sporozoites were able to traverse (Figure
415 5A) and invade (Figure 5B) *in vitro* cultured HC-04 cells with comparable efficacy to Pf_WT
416 sporozoites. Moreover, Pf_AZMR sporozoites harboured intact apicoplasts (data not shown),
417 unlike the *P. berghei* azithromycin resistant parasites, which mostly lack a distinct apicoplast
418 (Figure 3B).
419
420 To mimic the *in vivo* life cycle phenotyping performed with azithromycin resistant *P. berghei*
421 parasites, we infected humanised mice—with chimeric livers containing mostly human and some
422 mouse hepatocytes—with Pf_AZMR sporozoites. Livers from humanised mice infected with
423 either Pf_WT (n=2 mice) or Pf_AZMR (n=3 mice) sporozoites were harvested at day 5 post
424 sporozoite IV inoculation and analysed by qRT-PCR to determine i/ the level of liver chimerism,
425 and ii/ parasite loads. All mice had >75% human hepatocytes (data not shown), indicating a
426 uniform infection potential, yet there was an 80% drop in parasite load of Pf_AZMR parasites
427 compared to Pf_WT (Figure 5C). Thus, Pf_AZMR parasites have a significantly reduced capacity
428 to replicate in liver cells *in vivo*.
429
430 IFA on thin sections from these infected humanised mouse livers revealed defects in liver stage
431 schizont development of Pf_AZMR in comparison to Pf_WT parasites (Figure 5D, 5E). The
432 Pf_AZMR liver stage schizonts show little to no staining with either the cytosolic marker anti-
433 HSP70 or the parasitophorous vacuole marker anti-PTEX150 (Figure 5D), indicative of severe
434 overall morphological anomalies. Additionally, Pf_AZMR liver stage schizonts exhibit aberrant
435 nuclear staining with no clear individual nuclei (Figure 5D). Indeed, nuclei often appeared to be
436 aggregated (Figure 5E), reminiscent of the donut-shaped clusters of nuclei in *P. berghei*
437 azithromycin resistant liver stages (Figure 4E). Moreover, whilst the size of the liver stage
438 parasites was the same for Pf_AZMR in comparison to Pf_WT (Figure 5F), the azithromycin
439 resistant parasites had significantly fewer nuclei (Figure 5G). Apicoplast morphology is also
440 aberrant in Pf_AZMR late liver stage schizonts, with anti-ACP staining of Pf_AZMR revealing
441 their apicoplasts to be collapsed and poorly defined in comparison to Pf_WT (Figure 5E).
442
443 Based on these severe defects of gross morphology, nuclear proliferation/separation, and
444 apicoplast integrity for the Pf_AZMR parasites at liver stage, they appear to be experiencing severe
445 fitness costs attributable to the G76V Rpl4 mutation at day 5 of liver stage development.
446

CONCLUDING REMARKS

Rpl4 is a hotspot for macrolide resistance, particularly in plastids

Our four azithromycin selection regimens, across two *Plasmodium* species, all retrieved parasites with point mutations in the apicoplast-encoded ribosomal protein Rpl4. Mutations in Rpl4 are also associated with azithromycin resistance in other strains of *P. falciparum* (Goodman et al., 2013; Sidhu et al., 2007; Wilson et al., 2015), zoonotic infections of people with *Babesia microti* (Marcos & Wormser, 2023) in the plastid of the green alga *Chlamydomonas reinhardtii* (Bowers et al., 2003), and in various bacteria related to the ancestor of plastids (Canu et al., 2002; Ma et al., 2020). Mutations in Rpl4 thus seem to be a universal mechanism of resistance to azithromycin and closely related macrolides.

Why are apicoplast Rpl4 mutations so prevalent in malaria parasite azithromycin resistance? We previously argued that malaria parasite organelle genomes, which are multi copy (Wilson et al., 1992), are hotspots for resistance generation simply because more chances exist for mutations to arise than do in single copy nuclear genes (Goodman et al., 2017). Furthermore, organelle genomes could be heteroplasmic, allowing selection of pre-existing mutations by a drug to rapidly generate resistance, as likely occurs with atovaquone (Goodman et al., 2017). Moreover, several different Rpl4 mutations can confer azithromycin resistance (Figure 1F), somewhat akin to various different mutations in mitochondrial cytochrome *b* being able to confer atovaquone resistance (Siregar et al., 2008; Syafruddin et al., 1999), which provides higher mathematical probability of resistance arising in a particular gene. Whatever the case, the frequency of Rpl4 mutations in resistance to azithromycin, both in this and other studies, demonstrates that apicoplast Rpl4 is a hotspot for azithromycin resistance. Sequencing Rpl4 should be a first point-of-call for surveillance of malaria parasite azithromycin resistance.

Rpl4 mutations confer fitness advantage to parasites under drug pressure during the asexual, blood stages, but fitness deficits for transmission

Drug pressure is intermittent across the malaria parasite life cycle. Most drugs target the asexual blood phase in the vertebrate host, yet drug pressure subsides when parasites progress through their sexual cycle in the mosquito. Pressure can recommence if the parasites make it back into a new human host using antimalarials. At this point, a resistance-conferring mutation becomes an obvious selective advantage again, but the resistance allele(s) must transit the mosquito stages and the human liver to achieve transmission (and ultimately spread) of resistance. The fitness landscape for a parasite gene thus changes quite dramatically across the parasite life cycle.

Both *P. berghei* and *P. falciparum* are dependent on their apicoplast during mosquito stage development (Biddau et al., 2021; Charan et al., 2017; Korbmacher et al., 2020; Rizopoulos et al., 2016; van Schaijk et al., 2014), and we set out to determine if mutations in apicoplast genes impacted parasite fitness in mosquitoes. Here, we showed that mutations conferring resistance to azithromycin (selected for by drug pressure during the blood phase) have differring consequences on fitness during mosquito phases. In *P. berghei,* the fitness deficit is severe in mosquito stages such as oocyst development and sporozoite production. However, in *P. falciparum* a different mutation in the same gene created no detectable fitness cost to the human parasite in mosquitoes. Whether this difference between *P. berghei* and *P. falciparum* azithromycin resistant parasites in mosquito stage fitness is due to them having different Rpl4 point mutations (G95D or S89L in *P.*

492 *berghei* versus G76V in *P. falciparum*; Figure 1E), or is based on some overarching difference in
493 how reliant each parasite species is on its apicoplast in mosquitoes is uncertain. Indeed, based on
494 the essentiality of apicoplast fatty acid biosynthesis for mosquito phase development in *P.*
495 *falciparum* (van Schaijk et al., 2014) but not rodent malaria species (Pei et al., 2010; Vaughan et
496 al., 2009; Yu et al., 2008), one might expect *P. berghei* with a sub-optimal apicoplast to cope better
497 in mosquitoes. However, that was not the case for *P. berghei* Rpl4 mutants phenotyped here, all
498 of which exhibited marked reduction in fitness in mosquitoes.
499
500 If a mutant parasite is able to complete the mosquito life cycle stages, and sporozoites accumulate
501 in the mosquito salivary glands, its next phase—after being delivered by a bite—is to find and
502 infect the vertebrate liver. Again, drug resistance mutations undergo selection for sufficient fitness
503 during this liver phase. Interestingly, there is a convergence of phenotypes between *P. berghei* and
504 *P. falciparum* azithromycin resistant parasites at late liver stage, both having defective apicoplasts
505 and reduced/abnormal nuclei biogenesis. The malaria parasite liver stage is tremendously
506 proliferative with extremely high metabolic demands (Lahree et al., 2023), and our phenotyping
507 indicates that a putatively sub-optimal apicoplast translation apparatus is apparently a major
508 impediment to liver development of both *P. berghei* and *P. falciparum*, *in vitro* and *in vivo*.
509
510 In *P. berghei*, the combined burden of poor/abnormal growth in mosquitoes and liver of
511 azithromycin resistant parasites blocked transmission, except where we provided massive
512 mechanical intervention. In *P. falciparum*, a severe detrimental effect in the liver stage *in vivo* in
513 humanised mice predicts a severe impairment of transmission. Whilst we were unable to test
514 whether the Pf_AZMR parasites are competent to progress from liver stage to blood stage and thus
515 achieve transmission, it seems likely that the *P. falciparum* azithromycin resistant mutant—despite
516 performing better in mosquitoes—will nevertheless experience impediments to transmission.
517 Whether or not the G76V mutation will block or reduce transmission of azithromycin resistance
518 in a real-world setting is not yet possible to say, but the indications are that the mutation will not
519 circulate freely, which should ultimately result in reduced transmission of azithromycin resistance,
520 which gives azithromycin one more desirable characteristic as a potential partner drug.
521 Refractoriness to spread of resistance would also mean that use of azithromycin for prophylaxis
522 might pose less of a risk for resistance selection than is commonly assumed.
523

524 **MATERIALS & METHODS**
525
526 **Experimental animals and parasites**
527 Male Swiss Webster mice, between 3 and 12 weeks old, were used in all experiments. Animals
528 were sourced from Monash Animal Research Platform. All animal experiments were in
529 accordance to the Prevention of Cruelty to Animals Act 1986 and the Prevention of Cruelty to
530 Animals Regulations 2008 and reviewed and were permitted by the Melbourne University
531 Animal Ethics Committee (Ethics IDs 1613928.1, 1714169, 1914889.1). Animals were
532 anaesthetised using ketamine/xylazine and euthanised via slow fill carbon dioxide followed by
533 cervical dislocation. *Plasmodium berghei* ANKA strain parasites were used in all experiments
534 both as a reference wild type (WT) line and to generate all subsequent drug resistant parasite
535 lines. *P. falciparum* NF54 strain parasites were used to generate all *P. falciparum* drug resistant
536 parasite lines. Adult female *Anopheles stephensi* mosquitoes (MR4) were used in all experiments
537 and reared under standard insectary conditions. Adult mosquitoes were grown at 27°C in 80%
538 humidity, with a light/dark cycle of 14:10 hours. Mosquito infections were performed in dark
539 conditions, and infected mosquitoes were maintained on 10% (v/v) sucrose.
540
541 **Drugs**
542 Azithromcyin was obtained from Sigma-Aldrich (Merck, NSW Australia), as pure
543 pharmaceutical secondary standards. Azithromycin was provided as a dihydrate (CAS Number:
544 117772-70-0) and administered once per day (q.d.) for 4 days as a suspension in PEG400 (MP
545 Biomedicals, Ohio, CAS Number 25322-68-3) via oral gavage (OG). Drug dilutions were made
546 fresh for each dosing experiment from identical drug batches as determined by LOT numbers.
547
548 **Activity of drugs *in vivo***
549 To test for the curative dose and to confirm the efficacy and tolerance of each drug, an initial *in*
550 *vivo* drug dosing assay was performed. Briefly, a donor mouse was pre-infected with *P. berghei*
551 ANKA parasites via intraperitoneal (IP) injection of frozen stock. Once the donor mouse reached
552 5% parasitaemia, it was euthanised and infected blood collected via cardiac puncture. Infected
553 blood was diluted in RPMI 1640 medium (Gibco, Cat no. 61870-036) + 10% foetal bovine
554 serum (Gibco, Cat no. 10100147) to a concentration of $1x10^7$ infected red blood cells (iRBC) per
555 200 µL. Two cohorts of three mice (placebo/vehicle treated [n=3] and drug treated [n=3]) were
556 infected with $1x10^7$ iRBC via intravenous (IV) tail vein injection on day 0. Once mice reached
557 2% parasitaemia (approximately day 3), they were treated with the placebo/vehicle or drug by
558 OG or IP injection (on days 3-6) and monitored daily by Giemsa (10% [v/v]) stained thin blood
559 smears to determine parasite clearance. Mice were further monitored for health by daily weight
560 measurements.
561
562 To evaluate the reported schizontocidal activity, dosing range and dosing methods of
563 azithromycin, and to determine the 50% and 90% effective doses (ED50 and ED90 respectively)
564 a Peters' four-day suppressive test (Peters, 1965) was performed. Two donor mice were pre-
565 infected with WT *P. berghei* ANKA parasites via IP injection of fresh blood from a P0 infection.
566 Once the donor mice reached approximately 5% parasitaemia, they were euthanised and infected
567 blood collected via cardiac puncture. Infected blood from both mice was mixed and diluted in
568 RPMI 1640 medium + 10% foetal bovine serum to a concentration of $1x10^7$ iRBC per 200 µL.
569 Seven cohorts of four mice were infected with $1x10^7$ iRBC via IV tail vein injection on day 0.

570 All seven cohorts were administered the vehicle (200 µL PEG400) as a control or a given
571 concentration of azithromycin (5 mg/kg, 15 mg/kg, 30 mg/kg, 45 mg/kg, 60 mg/kg, 70 mg/kg in
572 200 µL PEG400) q.d. by OG on days 0-3, with the initial dose on day 0 given 4 hours post-
573 infection (pi). Parasitaemia was measured on day 4 by Giemsa-stained thin blood smears to
574 determine percentage suppression in comparison to the untreated control. Mice were also
575 monitored daily for health and to confirm parasites were being cleared. Percentage suppression
576 (PS) of parasitaemia was calculated using the formula: $PS=100 \times ([C_{AV}-T]/C_{AV})$, where C_{AV}=
577 average parasitaemia in the control group, and T=parasitaemia of each treated replicate. Each PS
578 replicate was then plotted against the dose, and a non-linear regression curve was fitted using
579 GraphPad Prism 9 (Version 9.1.0) to determine the ED50 and ED90 doses of azithromycin.
580

581 **Generating drug resistant *P. berghei* parasites**

582 Selection of resistant *P. berghei* parasites *in vivo* was performed in the same way for each drug.
583 After inoculation via IV injection with $1x10^7$ iRBCs from a WT *P. berghei* ANKA infected
584 donor mouse, mice were treated with a clearance dose of the drug (60 mg/kg or 70 mg/kg
585 azithromycin) administered as described above. Mice were monitored daily by Giemsa-stained
586 thin blood smears, and once recrudescence was observed and parasitaemia reached
587 approximately 1-2%, mice were treated with another clearance dose of the drug. Parasites were
588 occasionally passaged into naïve mice should an immune response appear to have been
589 suppressing growth. This recrudescence→treatment→recrudescence→treatment cycle was
590 repeated until parasitaemia failed to reduce in the presence of the drug, at which point parasites
591 were deemed resistant and parasite lines were cloned by limiting dilution. Cloned lines were then
592 confirmed to be resistant to the clearance dose by performing an *in vivo* drug assay as described
593 above.
594

595 **Generating drug resistant *P. falciparum* parasites**

596 NF54 and 3D7 parasites were cloned by limiting dilution prior to resistance generation. Two
597 independent clones of NF54 and one of 3D7 were used for selection. Parasite cultures containing
598 $5x10^8$ parasites were treated continuously for 96 hours with 300 nM azithromycin or 72 hours
599 with 30 nM atovaquone, or 200 nM pyrimethamine. All three parasite lines were also grown
600 without drug as a sequencing control. Following treatment, cultures were allowed to recover in
601 drug free media until recrudescence (24 days post azithromycin treatment, 30-38 days post
602 atovaquone treatment, and 24-29 days post pyrimethamine treatment). Drug was reapplied to
603 recrudescent parasites at the initial concentration. For azithromycin resistance, parasites grew
604 normally up to 600 nM azithromycin and survived with signicantly impaired growth at
605 concentrations up to 1.2 µM. Atovaquone and pyrimethamine resistant parasites required from
606 two to five cycles of treatment and recovery before stable drug resistance at three times the initial
607 concentrations was obtained. Resistance parasites were cloned by limiting dilution, and drug
608 resistance confirmed by standard SYBRgreen drug assays. DNA was prepared from independent
609 clones for whole genome sequening.
610

611 **Genomic DNA preparation and initial sequence analysis**

612 Whole blood was collected via cardiac puncture from mice infected with clonal drug resistant *P.*
613 *berghei* parasite lines, and 10 µL aliquots were transferred into 190 µL dPBS for a total volume
614 of 200 µL. Genomic DNA was extracted using an Isolate II Genomic DNA Kit (Bioline,
615 Meridian Bioscience Australia), following the manufacturer's instructions. Known loci

616 potentially involved in resistance to azithromycin amplified by polymerase chain reaction (PCR)
617 for targeted sequencing (See Supplementary Table 1. for primer sequences and PCR conditions).
618 Correct sized amplicons were then purified using an Isolate II PCR and Gel Kit (Bioline,
619 Meridian Biosciences, Australia) following the manufacturer's instructions for PCR clean-up and
620 sent for Sanger sequencing at the Victorian Clinical Genetics Services (VCGS; Murdoch
621 Children's Research Institute, Royal Children's Hospital, Parkville, Victoria) following their
622 purified DNA criteria. Alignment and analysis of sequenced amplicons was done using
623 Sequencher (Gene Codes Corporation, USA).
624

625 **Sample preparation and genomic DNA extraction for Illumina sequencing**

626 To obtain a concentrated, pure parasite sample, free of contaminant mouse leucocytes, platelets
627 and other material, we performed a *P. berghei* schizont preparation. Whole blood was collected
628 via cardiac puncture from mice infected with the clonal drug resistant *P. berghei* parasite lines,
629 and placed into a 50 mL overnight culture in complete schizont culture medium (70% [v/v]
630 RPMI 1640 medium, 30% [v/v] FBS and gentamycin (Gibco) $4x10^{-2}$ mg/mL). Approximately 20
631 hours post culture, schizonts were purified using a CS column (Miltenyi Biotec, Germany)
632 assembled in a VarioMACS magnetic cell separator (Miltenyi Biotec, Germany) and eluted in
633 RPMI 1640 medium. Purified schizonts were spun down in a swing-bucket centrifuge at 1500
634 RPM for 10 minutes, resuspended in 1 mL of dPBS, centrifuged again at 1500 RPM for 10
635 minutes and resuspended in 1 mL dPBS. Each 1 mL washed schizont preparation was then
636 distributed into five 200 µL aliquots and genomic DNA was extracted immediately using a
637 QIAmp DNA Blood Mini Kit (Qiagen) following the manufacturer's instructions with one
638 exception. After lysis at 56°C, preparations were centrifuged at maximum (13000 RPM) and
639 supernatant was placed into a new 1.5 mL tube to remove digested haemoglobin. After this step,
640 the protocol was followed verbatim. Samples were sent to the VCGS (Murdoch Children's
641 Research Institute, Royal Children's Hospital, Parkville, Victoria) for Illumina Nextera XT
642 library preparation and whole genome sequencing on either an Illumina HiSeq4000 or NovaSeq2
643 (150 bp paired-end reads).
644

645 **Bioinformatic analysis**

646 Analyses were performed using the High Performance Computing Services at The University of
647 Melbourne (Parkville, Victoria) or personal computers. Raw FASTQ files were mapped to the *P.*
648 *berghei* ANKA or *P. falciparum* 3D7 reference genome (Version 43 (*P. berghei*), Version 44 (*P.*
649 *falciparum*), PlasmoDB (Aurrecoechea et al., 2009)) using the Burrows-Wheeler Aligner (Li &
650 Durbin, 2009) and the quality checked with FastQC (Andrews, 2010) and QualiMap
651 (Okonechnikov et al., 2016). Mapped reads were visualised using Integrated Genomics Viewer
652 (IGV, version 2.8.4 (Thorvaldsdóttir et al., 2013)). Duplicate reads were marked using Picard
653 tools (version 2.18.27) MarkDuplicates tool. Variant calling was performed following the
654 Genome Analysis Toolkit (GATK)(McKenna et al., 2010) best practices pipeline (Van der
655 Auwera et al., 2013), using the HaplotypeCaller (in GVCF mode) and GenotypeGVCFs tools.
656 Raw variants were then annotated using SnpEff (Cingolani et al., 2012) and filtered using
657 SnpSift (Ruden et al., 2012) based on quality scores, read depth and genome position (i.e.
658 intergenic versus coding regions). Further manual filtering and analysis was performed using
659 GNU/Linux coreutils and Awk programming language (Aho et al., 1979) based on biological
660 relevance.
661

662 **Infection of mosquitoes with *P. berghei***
663 Female *A. stephensi* mosquitoes were infected with clonal *P. berghei* drug resistant lines and WT
664 *P. berghei* ANKA to investigate the fitness, phenotype and transmissibility of drug resistant
665 parasites. Approximately 200 µL frozen blood stock was used to infect a donor mouse by IP
666 injection. Once parasitaemia reached between 5-8% parasite readiness for infection was
667 confirmed by checking for exflagellation of microgametes by microscopy. Donor mice were then
668 anaesthetised, and individually placed on an infection cage containing 100 female *A. stephensi*
669 mosquitoes, which were allowed to feed for up to 40 minutes in a 20°C incubator at 80%
670 humidity. The donor mouse was euthanised post feed. Infected mosquitoes were maintained on
671 10% (v/v) sucrose for up to 28 days, or when the experiment was ended.
672
673 **Oocyst quantification and immunofluorescence assays**
674 Whole midguts were dissected from infected mosquitoes between 9- and 14-days post blood feed
675 and either stained with 0.2% (v/v) mercurochrome to assess oocyst numbers, or prepared for
676 immunofluorescence assay. In 24-well plates, whole midguts were dissected in dPBS and then
677 fixed in 4% (v/v) paraformaldehyde in dPBS for 1 hour at room temperature. After washing in 1
678 mL fresh dPBS three times for 5 minutes on an orbital shaker, midguts were blocked and
679 permeabilised overnight at 4°C in midgut blocking buffer (0.25% [v/v] Triton X-100, 5% [w/v]
680 BSA [Sigma-Aldrich, Cat no. A4503-50G] in dPBS). Midguts were incubated with primary
681 antibodies (apicoplast marker acyl carrier protein [ACP] anti-serum (Waller et al., 2000) at
682 1:250) diluted in midgut blocking buffer for a minimum of 4 hours at room temperature on an
683 orbital shaker. After washing three times in 1 mL dPBS, midguts were incubated at room
684 temperature for 2 hours on an orbital shaker with secondary antibodies (goat anti-rabbit IgG
685 Alexa Fluor 488 [Abcam] at 1:4000) diluted in midgut blocking buffer. Midguts were then
686 washed three times for 5 minutes in 1 mL dPBS on an orbital shaker, with the second wash
687 containing Hoechst 33342 diluted to 1:10 000 and mounted on glass slides in Dako fluorescence
688 mounting medium. Immunofluorescence assays were imaged on a Nikon C2 confocal
689 microscope and images assembled in ImageJ Fiji (Version 2.1.0/1.53c) (Schindelin et al., 2012).
690
691 **Quantitative PCR for organellar genome detection**
692 Primers designed to target genes encoded in the nuclear, apicoplast and mitochondrial genomes
693 (See Supplementary Table 1. for primer sequences and qPCR conditions) were used to perform
694 quantitative PCR (qPCR) on oocyst stage parasites isolated as described above. All primers were
695 first tested to ensure similar amplification efficiency under the assay conditions by generating
696 standard curves (Supplementary Figure 1.). Genomic DNA was extracted from parasite lines
697 using an Isolate II Genomic DNA Kit (Bioline, Meridian Bioscience Australia), following the
698 manufacturer's instructions, with one exception. Whole midguts were first dissected into 180 µL
699 lysis buffer GL (Bioline) and 20 µL Proteinase K and incubated at 56°C for 1 hour to ensure
700 efficient lysis of oocysts, the original protocol was then followed verbatim. All qPCR assays
701 were performed on a CFX Connect Real-Time PCR Detection System (Bio-Rad). Genome copy
702 number was calculated using the $\Delta\Delta C_T$ method (Livak & Schmittgen, 2001), first normalising
703 mean C_T values of apicoplast and mitochondrial genes within samples to the mean C_T of the
704 nuclear genes, then using the WT *P. berghei* ANKA samples as a calibrator for the drug resistant
705 lines.
706

707 **Sporozoite quantification and immunofluorescence motility assays**
708 Eight-well chamber slides (Merck Millipore Cat no. PEZGS0816) were coated with either
709 mouse-derived monoclonal circumsporozoite protein (CSP) anti-serum (1:1000) (Yoshida et al.,
710 1980) or mouse-derived polyclonal *P. berghei* anti-serum (1:1000; made in our laboratory)
711 diluted in dPBS, and incubated at 37°C for 1 hour. Salivary glands were dissected in 1640
712 medium + 10% foetal bovine serum from infected mosquitoes between 20- and 24-days post
713 blood feed, and purified sporozoites were counted. After removing the coating antibody solution
714 from the chamber slide, up to $2x10^4$ sporozoites from each drug resistant *P. berghei* parasite line
715 or WT *P. berghei* ANKA were added to individual wells and allowed to settle and glide for 1
716 hour at 37°C. The supernatant was then removed and parasites fixed with 150 µL of 4% (v/v)
717 paraformaldehyde in dPBS for 20 minutes at room temperature. After washing gently with dPBS
718 three times for 5 minutes, blocking buffer (0.2% [v/v] Triton X-100, 3% [w/v] BSA in dPBS)
719 was added to each well and left to incubate for 20 minutes at room temperature. Primary
720 antibodies were then added to each well (mouse anti-CSP [1:500], mouse anti-*P. berghei* [1:500]
721 or rabbit anti-ACP [1:250] as described above) diluted in 3% (w/v) BSA in dPBS. Wells were
722 again washed three times for 5 minutes with dPBS before incubating with secondary antibodies
723 (goat anti-rabbit IgG Alexa Fluor 488 [Abcam]; goat anti-mouse IgG Alexa Fluor 568 [Abcam])
724 diluted in 3% (w/v) BSA (all 1:2000). Wells were then washed three times for 5 minutes in
725 dPBS, with the second wash containing Hoechst 33342 diluted to 1:10000, and mounted with
726 Dako fluorescence mounting medium. Sporozoites were then imaged on a Leica DM6000B
727 compound fluorescence microscope and images assembled in ImageJ Fiji (Version 2.1.0/1.53c)
728 (Schindelin et al., 2012).
729
730 **Mosquito infection and analysis of parasite development**
731 Seven-day old female *Anopheles stephensi* mosquitoes (originally provided by M. Jacobs-
732 Lorena, John Hopkins University) were allowed to feed on asynchronous gametocytes at 0.6%
733 stage V gametocytemia using water jacketed glass membrane feeders. Mosquitos were then
734 sugar starved for 48 hours to kill any that had not fed or males. Those that survived were given
735 di-ionised water through cotton wicks and sugar cubes. For oocyst quantification; midguts were
736 dissected from ethanol killed mosquitos 7 days post feed and stained with 0.1% mercurochrome.
737 Salivary glands were dissected for mosquitos 16 days post feed, crushed with a pestle, and then
738 filtered through glass wool. Sporozoites were counted using a hemocytometer.
739
740 **Infection of naïve mice with *P. berghei* sporozoites and analysis of infectivity**
741 Naïve mice were infected with drug resistant or WT *P. berghei* ANKA sporozoites either by IV
742 tail vein injection or by direct blood feeding. For IV infection, salivary glands were dissected
743 from infected mosquitoes between days 20 and 24 post blood feed directly into RPMI 1640
744 medium + 10% (v/v) FBS. Sporozoites were then purified and counted prior to injecting either
745 $1x10^3$ or $1x10^4$ sporozoites per mouse. For direct blood feed, infected mosquitoes were allowed
746 to bite anaesthetised naïve mice. A total of 15 mosquitoes were allowed to blood feed for 15
747 minutes or until fed. Parasitaemia of mice was monitored by Giemsa-stained thin blood smears
748 from day 2 post IV or mosquito bite to assess blood stage patency.
749
750 **Liver stage development analysis *in vitro***
751 To investigate the development of parasites through the liver stage, human hepatoma HepG2
752 (ATCC No. HB-8065) or HC-04 (ATCC MRA-975) cell lines were cultured at 37°C and 5%

753 CO_2 in a T-25 culture flask (Corning) in HepG2 medium (Advanced MEM minus L-Glutamine
754 [Gibco] + 10% [v/v] HI-FBS [Gibco] + 1% [v/v] penicillin-streptomycin + 2 mM Glutamax
755 [Gibco] and 0.1% [v/v] amphotericin B). Once the HepG2 or HC-04 cells were grown to the
756 desired concentration, $1x10^5$ to $2x10^5$ cells were seeded onto coverslips in a 24-well plate in 1
757 mL HepG2 medium per well. The following day, sporozoites were dissected directly into HepG2
758 medium, purified and counted and up to $2x10^4$ sporozoites were added into each well and
759 allowed to settle and invade for 2 hours at 37°C and 5% CO_2. Media was changed after the 2-
760 hour invasion process, and then twice daily thereafter until cells were fixed. Infected HepG2 or
761 HC-04 cells were fixed on the coverslips for 20 minutes with 4% (v/v) paraformaldehyde in
762 dPBS, at either 24- or 48-hours post sporozoite infection. Coverslips were washed with dPBS
763 three times for 5 minutes in the 24-well plate before adding 1 mL ice-cold methanol for storage
764 (no more than 3 weeks) at 20°C. After removing the methanol, coverslips were washed three
765 times for 5 minutes with dPBS before cells were permeabilised with 0.1% (v/v) Triton X-100 in
766 dPBS for 20 minutes at room temperature. Washing steps were repeated, and cells were then
767 blocked for 30 minutes at room temperature with 3% (w/v) BSA in dPBS. Coverslips were
768 incubated with primary antibodies (mouse anti-*P. berghei* [1:500] and rabbit anti-ACP [1:250])
769 and secondary antibodies (goat anti-rabbit IgG Alexa Fluor 488 [Abcam]; goat anti-mouse IgG
770 Alexa Fluor 568 [Abcam]) in 3% BSA in dPBS for one hour at room temperature, washing three
771 times for 5 minutes with dPBS in between each incubation. Following the probing with
772 secondary antibodies, coverslips were washed three times for 5 minutes in dPBS, with the second
773 wash containing Hoechst 33342 diluted to 1:10000 and mounted with Dako fluorescence
774 mounting medium on glass slides and sealed with clear nail polish. Infected HepG2 and HC-04
775 liver cells were imaged on a Nikon C2 confocal microscope, and images assembled and
776 measured in ImageJ Fiji (Version 2.1.0/1.53c) (Schindelin et al., 2012).
777
778 **Humanised mice processing**
779 FRG humanised mice were obtained from Yecuris. An inoculum of $8x10^5$ *P. falciparum* control
780 NF54 sporozoites and $8x10^5$ Azithromycin resistant sporozoites freshly isolated from mosquito
781 salivary glands were injected into each humanised mouse (2 mice infected with NF54 and 3 mice
782 with Azithromycin resistant lines).
783 Livers were obtained 5.5 days post infection from CO_2-euthanized mice, and individual lobes
784 were cut as described (Foquet et al., 2013). Half of the lobes were embedded in OCT and frozen
785 in liquid nitrogen for IFA analysis, while half was emulsified into a single-cell suspension and
786 frozen and -80 for subsequent gDNA extraction.

787 For quantification of parasite load in the chimeric livers of each mouse; gDNA was isolated from
788 the single-cell liver suspensions, and Taqman probe-based quantitative PCRs were performed as
789 previously described (Alcoser et al., 2011; Foquet et al., 2013; Lopaticki et al., 2017; Yang et al.,
790 2017) using primers that would specifically amplify the 18S gene in each parasite line 18S_fwd
791 (5' -GTAATTGGAATGATAGGAATTTACAGGT-3') and 18S_rev (5'-
792 TCAACTACGAACGTTTTAACTGCAAC-3'). Human and mouse genomes were quantified
793 using oligonucleotides specific for prostaglandin E receptor 2 (PTGER2) from each species, as
794 described (Alcoser et al., 2011). All probes were labelled 5' with the fluorophore 6-carboxy-
795 fluorescein (FAM) and contain a double quencher that includes and internal ZEN quencher and a
796 3' Iowa Black quencher from IDT.

797 The following probes were used:

798 18S: 5'FAM TGCCAGCAG/ZEN/CCGCGGTA-3IABkFQ

799 hPTGER2: FAM/TGCTGCTTC/ZEN/TCATTGTCTCG/3IABkFQ,

800 mPTGER2: FAM/CCTGCTGCT/ZEN/TATCGTGGCTG/3IABkFQ
801
802 Standard curves were prepared by titration of from a defined number of DNA copies for *P.*
803 *falciparum* NF54, human and mouse controls. PCRs were performed on a Roche LC80 using
804 LightCycler 480 Probes Master (Roche).
805
806 **Immunofluorescence assay**
807 Purified NF54 and azithromycin resistant sporozoites were fixed with 4% paraformaldehyde
808 (PFA)/ 0.0075% glutaraldehyde in PBS at room temperature for 20 minutes. Sporozoites were
809 permeabilised in 0.1% Triton X 100 for 10 minutes before being blocked in 3% BSA PBS for 1
810 hour at room temperature. Samples were incubated with primary antibodies; rabbit anti-ACP
811 antibody (1:500), and mouse anti-CSP 2A10 (1:1000), for 1 hour in 3% BSA PBS followed by
812 secondary antibodies; anti-mouse 488 and anti-rabbit 594 (1:1000, Invitrogen). Images of NF54
813 or azithromycin sporozoites were taken at random based on CSP and DAPI and presence or
814 absence of apicoplast was then determined by staining with ACP.

815 For liver stage immunofluorescence analysis; livers were perfused with 1x PBS and fixed in 4%
816 PFA PBS overnight before being exchanged for sucrose and snap frozen in OCT (Invitrogen).
817 Sections of 8 mm were cut on the cryostat apparatus HMM550. Samples were permeabilised
818 using ice cold 10% methanol 90% acetone and blocked using 3% BSA PBS. Sections were then
819 incubated with primary antibodies; mouse anti-CSP (2A10; 1:1000), mouse anti-HSP70 (1:500),
820 rabbit anti-PTEX150 (1:500), mouse anti-EXP2 (1:500), rabbit anti-ACP (1:500) diluted in 3%
821 BSA PBS. Secondary antibodies were goat anti-rabbit Alexa 594 and anti-mouse Alexa 488
822 (1:1000; Invitrogen). All samples were then incubated with DAPI (4',6'- diamidino-2-
823 phenylindole) at 1 ug/ml in PBS to visualize DNA and mounted in Prolong Gold mounting
824 media (Invitrogen). Images were acquired on the Zeiss LSM 980 microscope.

825 Z stacks of both NF54 and azithromycin resistant liver stages were acquired using the same
826 settings to allow quantitative analysis between different samples. The number of nuclear centres
827 were counted by eye based on DAPI signal at the centre of each Z stack. For analysis of parasite
828 size; a region of interest was drawn around each parasite based on DAPI signal and then the
829 membrane area was calculated using FIJI software.

830 **Traversal assay**
831 Cell traversal was measured using a cell wounding assay (Kaushansky et al., 2012). HC-04
832 hepatocytes ($1x10^5$) were seeded onto the bottom of a 96-well plate using IMDM (Life
833 Technologies, 11360-070). Sporozoites were added at an MOI of 0.3 and left to traverse
834 hepatocytes for 2.5 hours in the presence of 1 mg ml-1 FITC-labelled dextran (10,000 MW,
835 Sigma Aldrich). Cells were trypsinized to obtain a single cell suspension for FACS analysis. For

836 each condition, triplicate samples of 10,000 cells were counted by flow cytometry in each of the
837 three independent experiments.
838
839 **Invasion assay**
840 Assay was performed as previously described (Kaushansky et al., 2012). Briefly, HC-04
841 hepatocytes ($1x10^5$) were seeded onto the bottom of a 96-well plate using IMDM (Life
842 Technologies, 11360-070). Sporozoites were added at an MOI of 0.3 and left to invade
843 hepatocytes for either 5 or 18 hours before being trypsinized to obtain a single cell suspension
844 and transferred to a 96 well round bottom plate. Cells were fixed and permeabilised (BD
845 bioscience) and stained with Alexa fluor 647 conjugated mouse anti-CSP antibody in 3% BSA
846 permeabilizing solution. Cells were then washed in PBS and analysed by Flow cytometry. For
847 each condition, triplicate samples of 10,000 cells were counted in each of the three independent
848 experiments.
849
850
851

852 REFERENCES
853

854 Aho, A. V., Kernighan, B. W., & Weinberger, P. J. (1979). Awk—a pattern scanning and
855 processing language. *Software: Practice and Experience*, *9*(4), 267-279.
856 Alcoser, S. Y., Kimmel, D. J., Borgel, S. D., Carter, J. P., Dougherty, K. M., & Hollingshead, M.
857 G. (2011). Real-time PCR-based assay to quantify the relative amount of human and mouse
858 tissue present in tumor xenografts. *BMC biotechnology*, *11*, 1-8.
859 Andrews, S. (2010). FastQC: a quality control tool for high throughput sequence data. In:
860 Babraham Bioinformatics, Babraham Institute, Cambridge, United Kingdom.
861 Ashley, E. A., Dhorda, M., Fairhurst, R. M., Amaratunga, C., Lim, P., Suon, S., Sreng, S.,
862 Anderson, J. M., Mao, S., Sam, B., Sopha, C., Chuor, C. M., Nguon, C., Sovannaroth, S.,
863 Pukrittayakamee, S., Jittamala, P., Chotivanich, K., Chutasmit, K., Suchatsoonthorn, C., .
864 . . White, N. J. (2014). Spread of Artemisinin Resistance in Plasmodium falciparum
865 Malaria. *New England Journal of Medicine*, *371*(5), 411-423.
866 https://doi.org/10.1056/NEJMoa1314981
867 Aurrecoechea, C., Brestelli, J., Brunk, B. P., Dommer, J., Fischer, S., Gajria, B., Gao, X., Gingle,
868 A., Grant, G., Harb, O. S., Heiges, M., Innamorato, F., Iodice, J., Kissinger, J. C., Kraemer,
869 E., Li, W., Miller, J. A., Nayak, V., Pennington, C., . . . Wang, H. (2009). PlasmoDB: a
870 functional genomic database for malaria parasites. *Nucleic Acids Res*, *37*(Database issue),
871 D539-543. https://doi.org/10.1093/nar/gkn814
872 Balikagala, B., Fukuda, N., Ikeda, M., Katuro, O. T., Tachibana, S. I., Yamauchi, M., Opio, W.,
873 Emoto, S., Anywar, D. A., Kimura, E., Palacpac, N. M. Q., Odongo-Aginya, E. I., Ogwang,
874 M., Horii, T., & Mita, T. (2021). Evidence of Artemisinin-Resistant Malaria in Africa. *N*
875 *Engl J Med*, *385*(13), 1163-1171. https://doi.org/10.1056/NEJMoa2101746
876 Balta, V. A., Stiffler, D., Sayeed, A., Tripathi, A. K., Elahi, R., Mlambo, G., Bakshi, R. P.,
877 Dziedzic, A. G., Jedlicka, A. E., Nenortas, E., Romero-Rodriguez, K., Canonizado, M. A.,
878 Mann, A., Owen, A., Sullivan, D. J., Prigge, S. T., Sinnis, P., & Shapiro, T. A. (2023).
879 Transmissibility of clinically relevant atovaquone-resistant Plasmodium
880 falciparum by anopheline mosquitoes. *bioRxiv*, 2023.2002.2007.527535.
881 https://doi.org/10.1101/2023.02.07.527535
882 Biddau, M., Santha Kumar, T. R., Henrich, P., Laine, L. M., Blackburn, G. J., Chokkathukalam,
883 A., Li, T., Lee Sim, K., King, L., Hoffman, S. L., Barrett, M. P., Coombs, G. H., McFadden,
884 G. I., Fidock, D. A., Müller, S., & Sheiner, L. (2021). *Plasmodium falciparum* LipB
885 mutants display altered redox and carbon metabolism in asexual stages and cannot
886 complete sporogony in *Anopheles* mosquitoes. *International Journal for Parasitology*,
887 *51*(6), 441-453. https://doi.org/https://doi.org/10.1016/j.ijpara.2020.10.011
888 Botté, C. Y., Dubar, F., McFadden, G. I., Maréchal, E., & Biot, C. (2012). Plasmodium falciparum
889 Apicoplast Drugs: Targets or Off-Targets? *Chemical reviews*, *112*(3), 1269-1283.
890 https://doi.org/10.1021/cr200258w
891 Bowers, A. K., Keller, J. A., & Dutcher, S. K. (2003). Molecular markers for rapidly identifying
892 candidate genes in *Chlamydomonas reinhardtii*: ERY1 and ERY2 encode chloroplast
893 ribosomal proteins. *Genetics*, *164*(4), 1345-1353.
894 https://doi.org/papers3://publication/uuid/EC240932-692E-433B-8F68-16F2CCC749A4
895 Buchanan, H. D., Goodman, C. D., & McFadden, G. I. (2022). Roles of the apicoplast across the
896 life cycles of rodent and human malaria parasites [https://doi.org/10.1111/jeu.12947].

897 *Journal of Eukaryotic Microbiology*, *69*(6), e12947.
898 https://doi.org/https://doi.org/10.1111/jeu.12947
899 Burns, A. L., Sleebs, B. E., Siddiqui, G., De Paoli, A. E., Anderson, D., Liffner, B., Harvey, R.,
900 Beeson, J. G., Creek, D. J., Goodman, C. D., McFadden, G. I., & Wilson, D. W. (2020).
901 Retargeting azithromycin analogues to have dual-modality antimalarial activity. *BMC*
902 *biology*, *18*(1), 133. https://doi.org/10.1186/s12915-020-00859-4
903 Canu, A., Malbruny, B., Coquemont, M., Davies, T. A., Appelbaum, P. C., & Leclercq, R. (2002).
904 Diversity of ribosomal mutations conferring resistance to macrolides, clindamycin,
905 streptogramin, and telithromycin in *Streptococcus pneumoniae*. *Antimicrobial agents and*
906 *chemotherapy*, *46*(1), 125-131.
907 Centers for Disease Control and Prevention. (2013). *Guidelines for Treatment of Malaria in the*
908 *United States*. CDC.
909 Chandra, R., Ansah, P., Sagara, I., Sie, A., Tiono, A. B., Djimde, A. A., Zhao, Q., Robbins, J.,
910 Penali, L. K., & Ogutu, B. (2015). Comparison of azithromycin plus chloroquine versus
911 artemether-lumefantrine for the treatment of uncomplicated Plasmodium falciparum
912 malaria in children in Africa: a randomized, open-label study. *Malaria Journal*, *14*(1), 108.
913 https://doi.org/10.1186/s12936-015-0620-8
914 Charan, M., Choudhary, H. H., Singh, N., Sadik, M., Siddiqi, M. I., Mishra, S., & Habib, S. (2017).
915 [Fe-S] cluster assembly in the apicoplast and its indispensability in mosquito stages of the
916 malaria parasite [10.1111/febs.14159]. *The FEBS Journal*, *284*(16), 2629-2648.
917 https://doi.org/papers3://publication/doi/10.1111/febs.14159
918 Chaubey, S., Kumar, A., Singh, D., & Habib, S. (2005). The apicoplast of Plasmodium falciparum
919 is translationally active. *Molecular Microbiology*, *56*(1), 81-89.
920 https://doi.org/https://doi.org/10.1111/j.1365-2958.2005.04538.x
921 Cingolani, P., Platts, A., Wang, L. L., Coon, M., Nguyen, T., Wang, L., Land, S. J., Lu, X., &
922 Ruden, D. M. (2012). A program for annotating and predicting the effects of single
923 nucleotide polymorphisms, SnpEff: SNPs in the genome of *Drosophila melanogaster*
924 strain w1118; iso-2; iso-3. *Fly*, *6*(2), 80-92.
925 Conrad, M. D., Asua, V., Garg, S., Giesbrecht, D., Niaré, K., Smith, S., Namuganga, J. F., Katairo,
926 T., Legac, J., Crudale, R. M., Tumwebaze, P. K., Nsobya, S. L., Cooper, R. A., Kamya, M.
927 R., Dorsey, G., Bailey, J. A., & Rosenthal, P. J. (2023). Evolution of Partial Resistance to
928 Artemisinins in Malaria Parasites in Uganda. *N Engl J Med*, *389*(8), 722-732.
929 https://doi.org/10.1056/NEJMoa2211803
930 Dahl, E. L., & Rosenthal, P. J. (2007). Multiple Antibiotics Exert Delayed Effects against the
931 *Plasmodium falciparum* Apicoplast [10.1128/AAC.00527-07]. *Antimicrobial agents and*
932 *chemotherapy*, *51*(10), 3485-3490.
933 https://doi.org/papers3://publication/doi/10.1128/AAC.00527-07
934 Dahl, E. L., & Rosenthal, P. J. (2008). Apicoplast translation, transcription and genome
935 replication: targets for antimalarial antibiotics. *Trends in Parasitology*, *24*(6), 279-284.
936 Dao Duc, K., Batra, S. S., Bhattacharya, N., Cate, Jamie H. D., & Song, Yun S. (2019).
937 Differences in the path to exit the ribosome across the three domains of life. *Nucleic acids*
938 *research*, *47*(8), 4198-4210. https://doi.org/10.1093/nar/gkz106
939 Das, S., Saha, B., Hati, A. K., & Roy, S. (2018). Evidence of Artemisinin-Resistant Plasmodium
940 falciparum Malaria in Eastern India. *New England Journal of Medicine*, *379*(20), 1962-
941 1964. https://doi.org/10.1056/NEJMc1713777

942 Dondorp, A. M., Fairhurst, R. M., Slutsker, L., MacArthur, J. R., M.D., J. G. B., Guerin, P. J.,
943 Wellems, T. E., Ringwald, P., Newman, R. D., & Plowe, C. V. (2011). The Threat of
944 Artemisinin-Resistant Malaria. *New England Journal of Medicine*, *365*(12), 1073-1075.
945 https://doi.org/10.1056/NEJMp1108322
946 Ejigiri, I., Ragheb, D. R. T., Pino, P., Coppi, A., Bennett, B. L., Soldati-Favre, D., & Sinnis, P.
947 (2012). Shedding of TRAP by a Rhomboid Protease from the Malaria Sporozoite Surface
948 Is Essential for Gliding Motility and Sporozoite Infectivity. *PLoS Pathogens*, *8*(7),
949 e1002725. https://doi.org/10.1371/journal.ppat.1002725
950 Falkard, B., Kumar, T. R. S., Hecht, L.-S., Matthews, K. A., Henrich, P. P., Gulati, S., Lewis, R.
951 E., Manary, M. J., Winzeler, E. A., Sinnis, P., Prigge, S. T., Heussler, V., Deschermeier,
952 C., & Fidock, D. (2013). A key role for lipoic acid synthesis during *Plasmodium* liver stage
953 development [https://doi.org/10.1111/cmi.12137]. *Cellular Microbiology*, *15*(9), 1585-
954 1604. https://doi.org/https://doi.org/10.1111/cmi.12137
955 Fola, A. A., Feleke, S. M., Mohammed, H., Brhane, B. G., Hennelly, C. M., Assefa, A., Crudal,
956 R. M., Reichert, E., Juliano, J. J., Cunningham, J., Mamo, H., Solomon, H., Tasew, G.,
957 Petros, B., Parr, J. B., & Bailey, J. A. (2023). Plasmodium falciparum resistant to
958 artemisinin and diagnostics have emerged in Ethiopia. *Nat Microbiol*, *8*(10), 1911-1919.
959 https://doi.org/10.1038/s41564-023-01461-4
960 Foquet, L., Hermsen, C. C., van Gemert, G.-J., Libbrecht, L., Sauerwein, R., Meuleman, P., &
961 Leroux-Roels, G. (2013). Molecular detection and quantification of *Plasmodium*
962 *falciparum*-infected human hepatocytes in chimeric immune-deficient mice. *Malaria*
963 *Journal*, *12*(1), 1-8.
964 Goodman, C. D., Buchanan, H. D., & McFadden, G. I. (2017). Is the mitochondrion a good malaria
965 drug target? *Trends in Parasitology*, *33*(3), 185-193.
966 Goodman, C. D., & McFadden, G. I. (2013). Targeting apicoplasts in malaria parasites. *Expert*
967 *Opinion on Therapeutic Targets*, *17*(2), 167-177.
968 https://doi.org/10.1517/14728222.2013.739158
969 Goodman, C. D., Siregar, J. E., Mollard, V., Vega-Rodriguez, J., Syafruddin, D., Matsuoka, H.,
970 Matsuzaki, M., Toyama, T., Sturm, A., Cozijnsen, A., Jacobs-Lorena, M., Kita, K.,
971 Marzuki, S., & McFadden, G. I. (2016). Parasites resistant to the antimalarial atovaquone
972 fail to transmit by mosquitoes. *Science (New York, N.Y.)*, *352*(6283), 349-353.
973 https://doi.org/10.1126/science.aad9279
974 Goodman, C. D., Su, V., & McFadden, G. I. (2007). The effects of anti-bacterials on the malaria
975 parasite *Plasmodium falciparum*. *Molecular and Biochemical Parasitology*, *152*(2), 181-
976 191. https://doi.org/https://doi.org/10.1016/j.molbiopara.2007.01.005
977 Goodman, C. D., Useglio, M., Peiru, S., Labadie, G. R., McFadden, G. I., Rodriguez, E., &
978 Gramajo, H. (2013). Chemobiosynthesis of New Antimalarial Macrolides
979 [10.1128/AAC.01825-12]. *Antimicrobial agents and chemotherapy*, *57*(2), 907-913.
980 https://doi.org/papers3://publication/doi/10.1128/AAC.01825-12
981 Griffith, K. S., Lewis, L. S., Mali, S., & Parise, M. E. (2007). Treatment of Malaria in the United
982 StatesA Systematic Review. *JAMA*, *297*(20), 2264-2277.
983 https://doi.org/10.1001/jama.297.20.2264
984 Hopp, C. S., Chiou, K., Ragheb, D. R. T., Salman, A. M., Khan, S. M., Liu, A. J., & Sinnis, P.
985 (2015). Longitudinal analysis of *Plasmodium* sporozoite motility in the dermis reveals
986 component of blood vessel recognition. *eLife*, *4*, e07789.
987 https://doi.org/10.7554/eLife.07789

988 Hyde, J. E. (2005). Exploring the folate pathway in Plasmodium falciparum. *Acta Tropica*, *94*(3),
989 191-206. https://doi.org/https://doi.org/10.1016/j.actatropica.2005.04.002
990 Imwong, M., Hien, T. T., Thuy-Nhien, N. T., Dondorp, A. M., & White, N. J. (2017). Spread of a
991 single multidrug resistant malaria parasite lineage (PfPailin) to Vietnam. *The*
992 *Lancet Infectious Diseases*, *17*(10), 1022-1023. https://doi.org/10.1016/S1473-
993 3099(17)30524-8
994 Jacot, D., & MacPherson, D. A. (2016). Apicomplexan Energy Metabolism: Carbon Source
995 Promiscuity and the Quiescence Hyperbole [10.1016/j.pt.2015.09.001]. *Trends in*
996 *Parasitology*, *32*(1), 56-70.
997 https://doi.org/papers3://publication/doi/10.1016/j.pt.2015.09.001
998 Kaushansky, A., Rezakhani, N., Mann, H., & Kappe, S. H. (2012). Development of a quantitative
999 flow cytometry-based assay to assess infection by *Plasmodium falciparum* sporozoites.
1000 *Molecular and Biochemical Parasitology*, *183*(1), 100-103.
1001 Ke, H., Sigala, P. A., Miura, K., Morrisey, J. M., Mather, M. W., Crowley, J. R., Henderson, J. P.,
1002 Goldberg, D. E., Long, C. A., & Vaidya, A. B. (2014). The heme biosynthesis pathway is
1003 essential for *Plasmodium falciparum* development in mosquito stage but not in blood
1004 stages. *J Biol Chem*, *289*(50), 34827-34837. https://doi.org/10.1074/jbc.M114.615831
1005 Kennedy, K., Cobbold, S. A., Hanssen, E., Birnbaum, J., Spillman, N. J., McHugh, E., Brown, H.,
1006 Tilley, L., Spielmann, T., McConville, M. J., & Ralph, S. A. (2019). Delayed death in the
1007 malaria parasite *Plasmodium falciparum* is caused by disruption of prenylation-dependent
1008 intracellular trafficking [10.1371/journal.pbio.3000376]. *PLoS Biology*, *17*(7), e3000376-
1009 3000328. https://doi.org/papers3://publication/doi/10.1371/journal.pbio.3000376
1010 Koehne, E., Adegnika, A. A., Held, J., & Kreidenweiss, A. (2021). Pharmacotherapy for
1011 artemisinin-resistant malaria. *Expert Opinion on Pharmacotherapy*, *22*(18), 2483-2493.
1012 https://doi.org/10.1080/14656566.2021.1959913
1013 Köhler, S., Delwiche, C. F., Denny, P. W., Tilney, L. G., Webster, P., Wilson, R., Palmer, J. D.,
1014 & Roos, D. S. (1997). A plastid of probable green algal origin in apicomplexan parasites.
1015 *Science*, *275*(5305), 1485-1489.
1016 Korbmacher, F., Drepper, B., Sanderson, T., Martin, P., Stach, T., Maier, A. G., Matuschewski,
1017 K., & Matz, J. M. (2020). An apicoplast-resident folate transporter is essential for
1018 sporogony of malaria parasites [10.1111/cmi.13266]. *Cellular Microbiology*, 1-35.
1019 https://doi.org/papers3://publication/doi/10.1111/cmi.13266
1020 Lahree, A., Mello-Vieira, J., & Mota, M. M. (2023). The nutrient games—*Plasmodium*
1021 metabolism during hepatic development. *Trends in Parasitology*.
1022 https://doi.org/10.1016/j.pt.2023.03.013
1023 Lell, B., & Kremsner, P. G. (2002). Clindamycin as an Antimalarial Drug: Review of Clinical
1024 Trials [10.1128/AAC.46.8.2315-2320.2002]. *Antimicrobial agents and chemotherapy*,
1025 *46*(8), 2315-2320. https://doi.org/papers3://publication/doi/10.1128/AAC.46.8.2315-
1026 2320.2002
1027 Li, H., & Durbin, R. (2009). Fast and accurate short read alignment with Burrows–Wheeler
1028 transform. *bioinformatics*, *25*(14), 1754-1760.
1029 Livak, K. J., & Schmittgen, T. D. (2001). Analysis of Relative Gene Expression Data Using Real-
1030 Time Quantitative PCR and the 2−ΔΔCT Method [10.1006/meth.2001.1262]. *Methods*,
1031 *25*(4), 402-408. https://doi.org/papers3://publication/doi/10.1006/meth.2001.1262
1032 Lopaticki, S., Yang, A. S., John, A., Scott, N. E., Lingford, J. P., O'Neill, M. T., Erickson, S. M.,
1033 McKenzie, N. C., Jennison, C., & Whitehead, L. W. (2017). Protein O-fucosylation in

Plasmodium falciparum ensures efficient infection of mosquito and vertebrate hosts. *Nature Communications*, *8*(1), 561.

Ma, K. C., Mortimer, T. D., Duckett, M. A., Hicks, A. L., Wheeler, N. E., Sánchez-Busó, L., & Grad, Y. H. (2020). Increased power from conditional bacterial genome-wide association identifies macrolide resistance mutations in *Neisseria gonorrhoeae*. *Nature Communications*, *11*(1), 5374. https://doi.org/10.1038/s41467-020-19250-6

Marcos, L. A., & Wormser, G. P. (2023). Relapsing Babesiosis With Molecular Evidence of Resistance to Certain Antimicrobials Commonly Used to Treat *Babesia microti* Infections. *Open Forum Infectious Diseases*, *10*(8). https://doi.org/10.1093/ofid/ofad391

McFadden, G. I., Reith, M. E., Munholland, J., & Lang-Unnasch, N. (1996). Plastid in human parasites. *Nature*, *381*, 482.

McFadden, G. I., & Yeh, E. (2017). The apicoplast: now you see it, now you don't. *International Journal for Parasitology*, *47*(2), 137-144. https://doi.org/https://doi.org/10.1016/j.ijpara.2016.08.005

McKenna, A., Hanna, M., Banks, E., Sivachenko, A., Cibulskis, K., Kernytsky, A., Garimella, K., Altshuler, D., Gabriel, S., & Daly, M. (2010). The Genome Analysis Toolkit: a MapReduce framework for analyzing next-generation DNA sequencing data. *Genome Research*, *20*(9), 1297-1303.

Ménard, D., & Fidock, D. A. (2019). Accelerated evolution and spread of multidrug-resistant Plasmodium falciparum takes down the latest first-line antimalarial drug in southeast Asia. *The Lancet Infectious Diseases*, *19*(9), 916-917. https://doi.org/10.1016/S1473-3099(19)30394-9

Nagaraj, V. A., Sundaram, B., Varadarajan, N. M., Subramani, P. A., Kalappa, D. M., Ghosh, S. K., & Padmanaban, G. (2013). Malaria Parasite-Synthesized Heme Is Essential in the Mosquito and Liver Stages and Complements Host Heme in the Blood Stages of Infection. *PLoS Pathogens*, *9*(8), e1003522. https://doi.org/10.1371/journal.ppat.1003522

Okonechnikov, K., Conesa, A., & García-Alcalde, F. (2016). Qualimap 2: advanced multi-sample quality control for high-throughput sequencing data. *bioinformatics*, *32*(2), 292-294.

Pei, Y., Tarun, A. S., Vaughan, A. M., Herman, R. W., Soliman, J. M. B., Erickson-Wayman, A., & Kappe, S. H. I. (2010). *Plasmodium* pyruvate dehydrogenase activity is only essential for the parasite's progression from liver infection to blood infection. *Molecular Microbiology*, *75*(4), 957-971. https://doi.org/10.1111/j.1365-2958.2009.07034.x

Peters, W. (1965). Drug resistance in *Plasmodium berghei* Vincke and Lips, 1948. I. Chloroquine resistance [10.1016/0014-4894(65)90012-3]. *Experimental parasitology*, *17*(1), 80-89. https://doi.org/papers3://publication/doi/10.1016/0014-4894(65)90012-3

Rathnapala, U. L., Goodman, C. D., & McFadden, G. I. (2017). A novel genetic technique in *Plasmodium berghei* allows liver stage analysis of genes required for mosquito stage development and demonstrates that de novo heme synthesis is essential for liver stage development in the malaria parasite [10.1371/journal.ppat.1006396]. *PLoS Pathogens*, *13*(6), e1006396-1006318. https://doi.org/papers3://publication/doi/10.1371/journal.ppat.1006396

Rizopoulos, Z., Matuschewski, K., & Haussig, J. M. (2016). Distinct Prominent Roles for Enzymes of *Plasmodium berghei* Heme Biosynthesis in Sporozoite and Liver Stage Maturation [10.1128/IAI.00148-16]. *Infection and Immunity*, *84*(11), 3252-3262. https://doi.org/papers3://publication/doi/10.1128/IAI.00148-16

1079 Rosenthal, P. J. (2016). Azithromycin for Malaria? *The American journal of tropical medicine and*
1080 *hygiene*, 16-0332.
1081 Ruden, D. M., Cingolani, P., Patel, V. M., Coon, M., Nguyen, T., Land, S. J., & Lu, X. (2012).
1082 Using *Drosophila melanogaster* as a model for genotoxic chemical mutational studies with
1083 a new program, SnpSift. *Frontiers in genetics*, *3*, 35.
1084 Sagara, I., Oduro, A. R., Mulenga, M., Dieng, Y., Ogutu, B., Tiono, A. B., Mugyenyi, P., Sie, A.,
1085 Wasunna, M., Kain, K. C., Djimdé, A. A., Sarkar, S., Chandra, R., Robbins, J., & Dunne,
1086 M. W. (2014). Efficacy and safety of a combination of azithromycin and chloroquine for
1087 the treatment of uncomplicated Plasmodium falciparum malaria in two multi-country
1088 randomised clinical trials in African adults. *Malaria Journal*, *13*(1), 458.
1089 https://doi.org/10.1186/1475-2875-13-458
1090 Schindelin, J., Arganda-Carreras, I., Frise, E., Kaynig, V., Longair, M., Pietzsch, T., Preibisch, S.,
1091 Rueden, C., Saalfeld, S., & Schmid, B. (2012). Fiji: an open-source platform for biological-
1092 image analysis. *Nature methods*, *9*(7), 676-682.
1093 Sidhu, A. B. S., Sun, Q., Nkrumah, L. J., Dunne, M. W., Sacchettini, J. C., & Fidock, D. A. (2007).
1094 In vitro efficacy, resistance selection, and structural modeling studies implicate the malarial
1095 parasite apicoplast as the target of azithromycin. *Journal of Biological Chemistry*, *282*(4),
1096 2494-2504.
1097 Siregar, J. E., Syafruddin, D., Matsuoka, H., Kita, K., & Marzuki, S. (2008). Mutation underlying
1098 resistance of Plasmodium berghei to atovaquone in the quinone binding domain 2 (Qo2)
1099 of the cytochrome b gene. *Parasitology International*, *57*(2), 229-232.
1100 https://doi.org/https://doi.org/10.1016/j.parint.2007.12.002
1101 Stanway, R. R., Bushell, E., Chiappino-Pepe, A., Roques, M., Sanderson, T., Franke-Fayard, B.,
1102 Caldelari, R., Golomingi, M., Nyonda, M., Pandey, V., Schwach, F., Chevalley, S.,
1103 Ramesar, J., Metcalf, T., Herd, C., Burda, P.-C., Rayner, J. C., Soldati-Favre, D., Janse, C.
1104 J., . . . Heussler, V. T. (2019). Genome-Scale Identification of Essential Metabolic
1105 Processes for Targeting the *Plasmodium* Liver Stage [10.1016/j.cell.2019.10.030]. *Cell*,
1106 *179*(5), 1112-1128.e1126.
1107 https://doi.org/papers3://publication/doi/10.1016/j.cell.2019.10.030
1108 Stanway, R. R., Witt, T., Zobiak, B., Aepfelbacher, M., & Heussler, V. T. (2009). GFP-targeting
1109 allows visualization of the apicoplast throughout the life cycle of live malaria parasites.
1110 *Biology of the Cell*, *101*(7), 415-435.
1111 Swift, R. P., Rajaram, K., Liu, H. B., & Prigge, S. T. (2021). Dephospho-CoA kinase, a nuclear-
1112 encoded apicoplast protein, remains active and essential after *Plasmodium falciparum*
1113 apicoplast disruption. *Embo Journal*, *40*, e107247.
1114 https://doi.org/10.15252/embj.2020107247
1115 Syafruddin, D., Siregar, J. E., & Marzuki, S. (1999). Mutations in the cytochrome b gene of
1116 Plasmodium berghei conferring resistance to atovaquone. *Molecular and Biochemical*
1117 *Parasitology*, *104*(2), 185-194. https://doi.org/https://doi.org/10.1016/S0166-
1118 6851(99)00148-6
1119 Thorvaldsdóttir, H., Robinson, J. T., & Mesirov, J. P. (2013). Integrative Genomics Viewer (IGV):
1120 high-performance genomics data visualization and exploration. *Briefings in*
1121 *bioinformatics*, *14*(2), 178-192.
1122 Uddin, T., McFadden, G. I., & Goodman, C. D. (2018). Validation of Putative Apicoplast-
1123 Targeting Drugs Using a Chemical Supplementation Assay in Cultured Human Malaria

Parasites. *Antimicrobial agents and chemotherapy*, *62*(1), e01161-01117. https://doi.org/10.1128/AAC.01161-17

Van der Auwera, G. A., Carneiro, M. O., Hartl, C., Poplin, R., del Angel, G., Levy-Moonshine, A., Jordan, T., Shakir, K., Roazen, D., Thibault, J., Banks, E., Garimella, K. V., Altshuler, D., Gabriel, S., & DePristo, M. A. (2013). *From FastQ Data to High-Confidence Variant Calls: The Genome Analysis Toolkit Best Practices Pipeline* (Vol. 467) [10.1002/0471250953.bi1110s43]. John Wiley & Sons, Inc. https://doi.org/papers3://publication/doi/10.1002/0471250953.bi1110s43

van der Pluijm, R. W., Amaratunga, C., Dhorda, M., & Dondorp, A. M. (2021). Triple Artemisinin-Based Combination Therapies for Malaria – A New Paradigm? *Trends in Parasitology*, *37*(1), 15-24. https://doi.org/10.1016/j.pt.2020.09.011

van Dooren, G. G., & Striepen, B. (2013). The Algal Past and Parasite Present of the Apicoplast. *Annual Review of Microbiology*, *67*(1), 271-289. https://doi.org/10.1146/annurev-micro-092412-155741

van Eijk, A. M., & Terlouw, D. J. (2011). Azithromycin for treating uncomplicated malaria. *Cochrane Database of Systematic Reviews*(2). https://doi.org/10.1002/14651858.CD006688.pub2

van Schaijk, B. C. L., Santha Kumar, T. R., Vos, M. W., Richman, A., van Gemert, G.-J., Eappen, A. G., Williamson, K. C., Morahan, B. J., Fishbaugher, M., Kennedy, M., Camargo, N., Khan, S. M., Janse, C. J., Sim, K. L., Hoffman, S. I., Kappe, S. H. I., Sauerwein, R. W., Fidock, D. A., & Vaughan, A. M. (2014). Type II fatty acid biosynthesis is essential for *Plasmodium falciparum* sporozoite development in the midgut of *Anopheles* mosquitoes. *Eukaryotic Cell*, *13*(5), 550-559. https://doi.org/10.1128/EC.00264-13

Vaughan, A. M., O'Neill, M. T., Tarun, A. S., Camargo, N., Phuong, T. M., Aly, A. S. I., Cowman, A. F., & Kappe, S. H. I. (2009). Type II fatty acid synthesis is essential only for malaria parasite late liver stage development. *Cellular Microbiology*, *11*(3), 506-520. https://doi.org/10.1111/j.1462-5822.2008.01270.x

Waller, R. F., Keeling, P. J., Donald, R. G. K., Striepen, B., Handman, E., Lang-Unnasch, N., Cowman, A. F., Besra, G. S., Roos, D. S., & McFadden, G. I. (1998). Nuclear-encoded proteins target to the plastid in *Toxoplasma gondii* and *Plasmodium falciparum*. *Proceedings of the National Academy of Sciences*, *95*(21), 12352-12357. https://doi.org/papers3://publication/uuid/615D8B7B-DC51-4759-9275-CE1223F52C74

Waller, R. F., Reed, M. B., Cowman, A. F., & McFadden, G. I. (2000). Protein trafficking to the plastid of *Plasmodium falciparum* is via the secretory pathway. *The EMBO Journal*, *19*(8), 1794-1802.

White, N. J. (2016). Can new treatment developments combat resistance in malaria? *Expert Opinion on Pharmacotherapy*, *17*(10), 1303-1307. https://doi.org/10.1080/14656566.2016.1187134

Wilson, D. W., Goodman, C. D., Sleebs, B. E., Weiss, G. E., de Jong, N. W. M., Angrisano, F., Langer, C., Baum, J., Crabb, B. S., Gilson, P. R., McFadden, G. I., & Beeson, J. G. (2015). Macrolides rapidly inhibit red blood cell invasion by the human malaria parasite, *Plasmodium falciparum* [10.1186/s12915-015-0162-0]. *BMC biology*, *13*(1), 1. https://doi.org/papers3://publication/doi/10.1186/s12915-015-0162-0

Wilson, R. J., Denny, P. W., Preiser, P. R., Rangachari, K., Roberts, K., Roy, A., Whyte, A., Strath, M., Moore, D. J., Moore, P. W., & Williamson, D. H. (1996). Complete gene map of the plastid-like DNA of the malaria parasite Plasmodium falciparum

1170 [10.1006/jmbi.1996.0449]. *Journal of Molecular Biology*, *261*(2), 155-172.
1171 https://doi.org/papers3://publication/doi/10.1006/jmbi.1996.0449
1172 Wilson, R. J., Fry, M., Gardner, M. J., Feagin, J. E., & Williamson, D. H. (1992). Subcellular
1173 fractionation of the two organelle DNAs of malaria parasites. *Current genetics*, *21*, 405-
1174 408.
1175 Yang, A. S., Lopaticki, S., O'Neill, M. T., Erickson, S. M., Douglas, D. N., Kneteman, N. M., &
1176 Boddey, J. A. (2017). AMA1 and MAEBL are important for *Plasmodium falciparum*
1177 sporozoite infection of the liver. *Cellular Microbiology*, *19*(9), e12745.
1178 Yeh, E., & DeRisi, J. L. (2011). Chemical Rescue of Malaria Parasites Lacking an Apicoplast
1179 Defines Organelle Function in Blood-Stage *Plasmodium falciparum*. *PLoS Biology*, *9*(8),
1180 e1001138. https://doi.org/10.1371/journal.pbio.1001138
1181 Yoshida, N., Nussenzweig, R. S., Potocnjak, P., Nussenzweig, V., & Aikawa, M. (1980).
1182 Hybridoma produces protective antibodies directed against the sporozoite stage of malaria
1183 parasite. *Science*, *207*(4426), 71-73.
1184 Yu, M., Kumar, T. R. S., Nkrumah, L. J., Coppi, A., Retzlaff, S., Li, C. D., Kelly, B. J., Moura, P.
1185 A., Lakshmanan, V., Freundlich, J. S., Valderramos, J.-C., Vilcheze, C., Siedner, M., Tsai,
1186 J. H. C., Falkard, B., Sidhu, A. B. S., Purcell, L. A., Gratraud, P., Kremer, L., . . . Fidock,
1187 D. A. (2008). The fatty acid biosynthesis enzyme FabI plays a key role in the development
1188 of liver-stage malarial parasites. *Cell Host & Microbe*, *4*(6), 567-578.
1189 https://doi.org/10.1016/j.chom.2008.11.001
1190

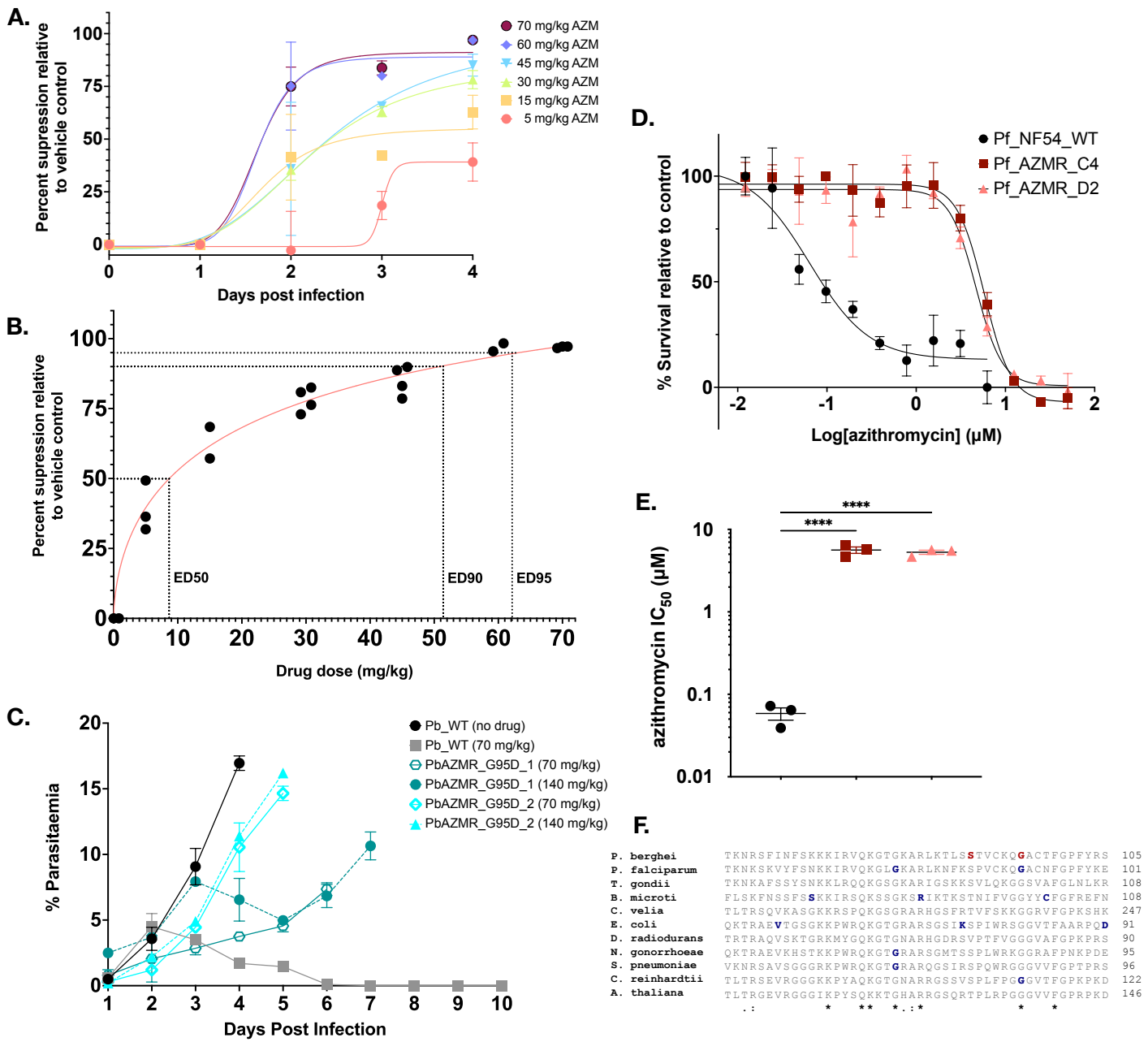

Figure 1. Summary drug assays performed *in vivo* with *P. berghei* and *in vitro* with *P. falciparum*. A.) Peters' four-day suppressive test *in vivo* with *P. berghei*. Percent suppression of a variable dosing range used to determine both the appropriate clearance dose and potential resistance-generating dose. Parasitaemias of individual mice in each dose cohort were normalised to the mean vehicle control-treated parasitaemia at each time point, and the mean percent-suppression value plotted (error bars represent ±SD). A non-linear regression curve with a variable slope was then fitted to the data points for each dose cohort; B.) End-point (day 4) data for the Peters' four-day suppressive test. Parasitaemias of individual mice in each dose cohort were normalised to the mean vehicle control-treated parasitaemia at day 4 and each individual value plotted. A non-linear regression curve with a variable slope was then fitted to the data points. Dotted lines indicate ED50 and ED90 values. Where n<4, mice were euthanised prior to

1203 the experimental end point for humane reasons; C.) *In vivo* drug assay of PbAZMR_G95D_1
1204 (teal) and PbAZMR_G95D_2 (light blue) grown with a full four-day 70 mg/kg q.d. (solid lines,
1205 n=2 per genotype) or 140 mg/kg q.d. (dashed lines, n=2 per genotype) drug course versus WT
1206 with the vehicle (no drug; black; n=2) and a full four-day 70 mg/kg q.d. drug course (grey; n=2).
1207 Both PbAZMR_G95D_1 and PbAZMR_G95D_2 parasites grow in the presence of either dose,
1208 while WT grows normally without drug, and is completely cleared of parasites by day 6 with
1209 treatment. Treatment was started on day 1. (Values indicate mean parasitaemia, and error bars
1210 represent the SEM); D.) Dose response curves of Pf_AZMR_C4 and Pf_AZMR_D2 clones (both
1211 with G76V mutation in *P. falciparum* 50S Rpl4) compared to Pf_WT. Data presented are the
1212 mean of three technical replicates and representative of three independent drug trials (error bars
1213 represent ±SD); E.) Comparison plot of IC50s of *P. falciparum* azithromycin resistant clones
1214 versus WT. Plotted are the mean IC50 values from three independent drug trials. (error bars
1215 represent the SEM, **** = P<0.0001, ordinary one-way ANOVA, Dunnett's multiple
1216 comparisons test); F.) Alignment of region of Rpl4 associated with azithromycin of
1217 erythromycin resistance in bacteria and plastids of parasites, algae and plants. Mutations
1218 identified in this study are depicted in red and mutations selected from the literature in blue.
1219 Included organisms: P. berghei (*Plasmodium berghei*); P. falciparum (*Plasmodium falciparum*);
1220 T. gondii (*Toxoplasma gondii*); B. microti (*Babesia microti*); C. velia (*Chromera velia*), E.coli
1221 (*Escherichia coli*); D. radiodurans (*Deinococcus radiodurans*); N. gonorrhoeae (*Neisseria*
1222 *gonorrhoeae*); S. pneumoniae (*Streptococcus pneumoniae*); C. reinhardtii (*Chlamydomonas*
1223 *reinhardtii*);A.thaliana (*Arabidopsis thaliana*). Asterisks denote invariant residues, colons depect
1224 conserved residues groups with strongly similar properties, and periods denote semi-conserved
1225 residues groups with similar properties.
1226
1227 (AZM = azithromycin; ED = effective dose)

1228

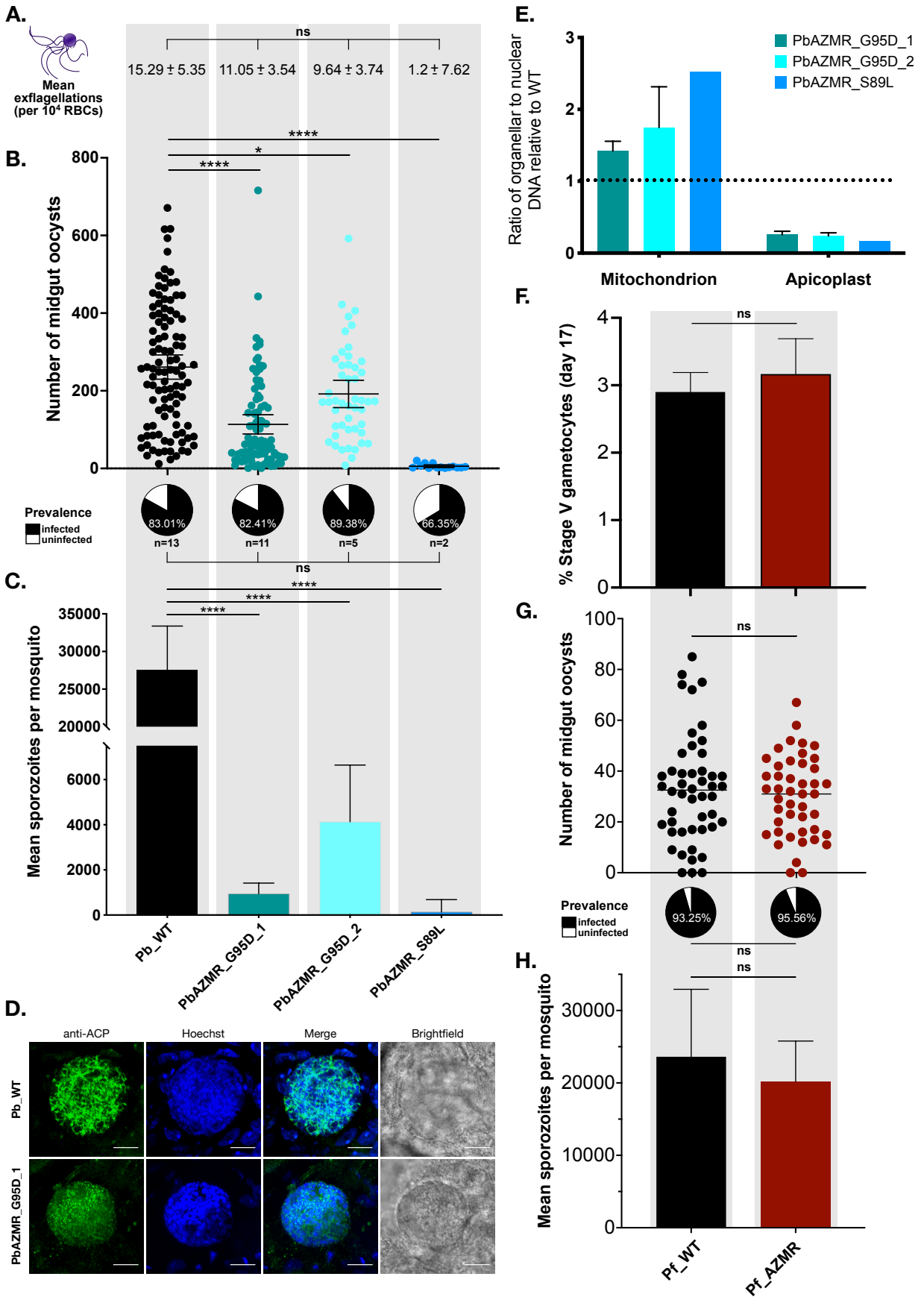
A.
Mean exflagellations (per 10⁴ RBCs)
ns
15.29 ± 5.35
11.05 ± 3.54
9.64 ± 3.74
1.2 ± 7.62
B.
Number of midgut oocysts
****
*
****
Prevalence
infected
uninfected
83.01%
82.41%
89.38%
66.35%
n=13
n=11
n=5
n=2
C.
Mean sporozoites per mosquito
ns
****
****
****
Pb_WT
PbAZMR_G95D_1
PbAZMR_G95D_2
PbAZMR_S89L
D.
anti-ACP
Hoechst
Merge
Brightfield
Pb_WT
PbAZMR_G95D_1
E.
Ratio of organellar to nuclear DNA relative to WT
PbAZMR_G95D_1
PbAZMR_G95D_2
PbAZMR_S89L
Mitochondrion
Apicoplast
F.
% Stage V gametocytes (day 17)
ns
G.
Number of midgut oocysts
ns
Prevalence
infected
uninfected
93.25%
95.56%
H.
Mean sporozoites per mosquito
ns
ns
Pf_WT
Pf_AZMR

1229 **Figure 2.** Mosquito infection data for both *P. berghei* and *P. falciparum* azithromycin resistant
1230 parasites. A.) Exflagellations were counted per $1x10^4$ red blood cells (RBCs) and are shown as
1231 the mean ±95%CI, with no significant difference between strains (ordinary one-way ANOVA
1232 with Dunnett's multiple comparisons; WT [n=17], PbAZMR_G95D_1 [n=20],
1233 PbAZMR_G95D_2 [n=10], PbAZMR_S89L [n=2], where 'n' is the number of independent
1234 biological replicates). At 9-to-14 days post blood feed, a minimum of 10 midguts were dissected
1235 for each independent infection (WT [n=13], PbAZMR_G95D_1 [n=11], PbAZMR_G95D_2
1236 [n=5], PbAZMR_S89L [n=2], where 'n' is the number of independent infections) and assessed
1237 for infection prevalence as a proportion of the total number of midguts dissected (pie charts
1238 below, percentage indicates the mean; ns= not significant by way of ordinary one-way ANOVA).
1239 Oocysts of infected midguts were counted and pooled, and non-zero values were plotted (error
1240 bars represent the mean ±95%CI). All azithromycin resistant strains had significantly fewer
1241 oocysts than WT (*=P<0.05; ****=P<0.0001; ordinary one-way ANOVA, Dunnett's multiple
1242 comparisons test), despite no significant difference in infectivity; B.) Mean number of salivary
1243 gland sporozoites per mosquito. Between days 20- and 26- post blood feed, a minimum of 12
1244 mosquitoes (WT) or 20 mosquitoes (PbAZMR_G95D_1, PbAZMR_G95D_2, and
1245 PbAZMR_S89L) were dissected and salivary glands isolated and sporozoites then counted. All
1246 azithromycin resistant strains produce fewer salivary gland sporozoites than WT
1247 (****=P<0.0001, Welch's t-test; error bar represents +95% CI). Results are from 'n'
1248 independent mosquito infections: WT (n=21), PbAZMR_G95D_1 (n=14), PbAZMR_G95D_2
1249 (n=10), PbAZMR_S89L (n=2); C.) Quantitative PCR on genomic DNA isolated from midguts
1250 infected with both *P. berghei* azithromycin resistant parasites and WT strains. Copy numbers of
1251 genes encoded in each organelle were first normalised to nuclear genes, before being expressed
1252 as a ratio to WT parasites. While there is variability in mitochondrial genome copy number, there
1253 is a clear reduction in apicoplast genome copy number in PbAZMR_G95D_1 (n=4),
1254 PbAZMR_G95D_2 (n=3) and PbAZMR_S89L (n=1), where n=number of biological replicates.
1255 Error bars represent the SEM; D.) Immunofluorescence assay on midgut oocysts, 14 days post
1256 blood feed. Green represents labelling of the *P. berghei* apicoplast, with anti-ACP antibodies.
1257 ACP is a protein encoded in the parasite nucleus and targeted to the apicoplast. Hoechst is
1258 staining DNA. PbAZMR_G95D_1 oocysts consistently show dispersed ACP staining (bottom
1259 panel), while WT oocysts show a branched ACP staining (top panel), typical of apicoplast
1260 development during oocyst maturation. Images are maximum projections (except brightfield,
1261 which shows the largest single slice). Scale bar=10μm; E.) Quantification of development of
1262 blood-feed-ready stage V gametocytes produced by Pf_WT and Pf_AZMR (clone C4) parasites.
1263 No significant difference is seen (Unpaired t-test, two-tailed P value); F.) At 7 days post blood
1264 feed, a minimum of 10 midguts were dissected for each independent infection (Pf_WT [n=3],
1265 Pf_AZMR [n=3]), where 'n' is the number of independent infections) and assessed for infection
1266 prevalence as a proportion of the total number of midguts dissected (pie charts below, percentage
1267 indicates the mean; ns= not significant by way of Unpaired t-test, two-tailed P value). No
1268 significant difference was observed between the number of midgut oocysts in mosquitoes
1269 infected with either Pf_WT or Pf_AZMR parasites (Unpaired t-test, two-tailed P value); G.) At
1270 day 17 post blood feed, a minimum of 12 mosquitoes were dissected per genotype, salivary
1271 glands isolated and sporozoites then counted. No significant difference was observed between
1272 the number of salivary gland sporozoites in mosquitoes infected with either Pf_WT or Pf_AZMR
1273 parasites (Unpaired t-test, two-tailed P value).
1274

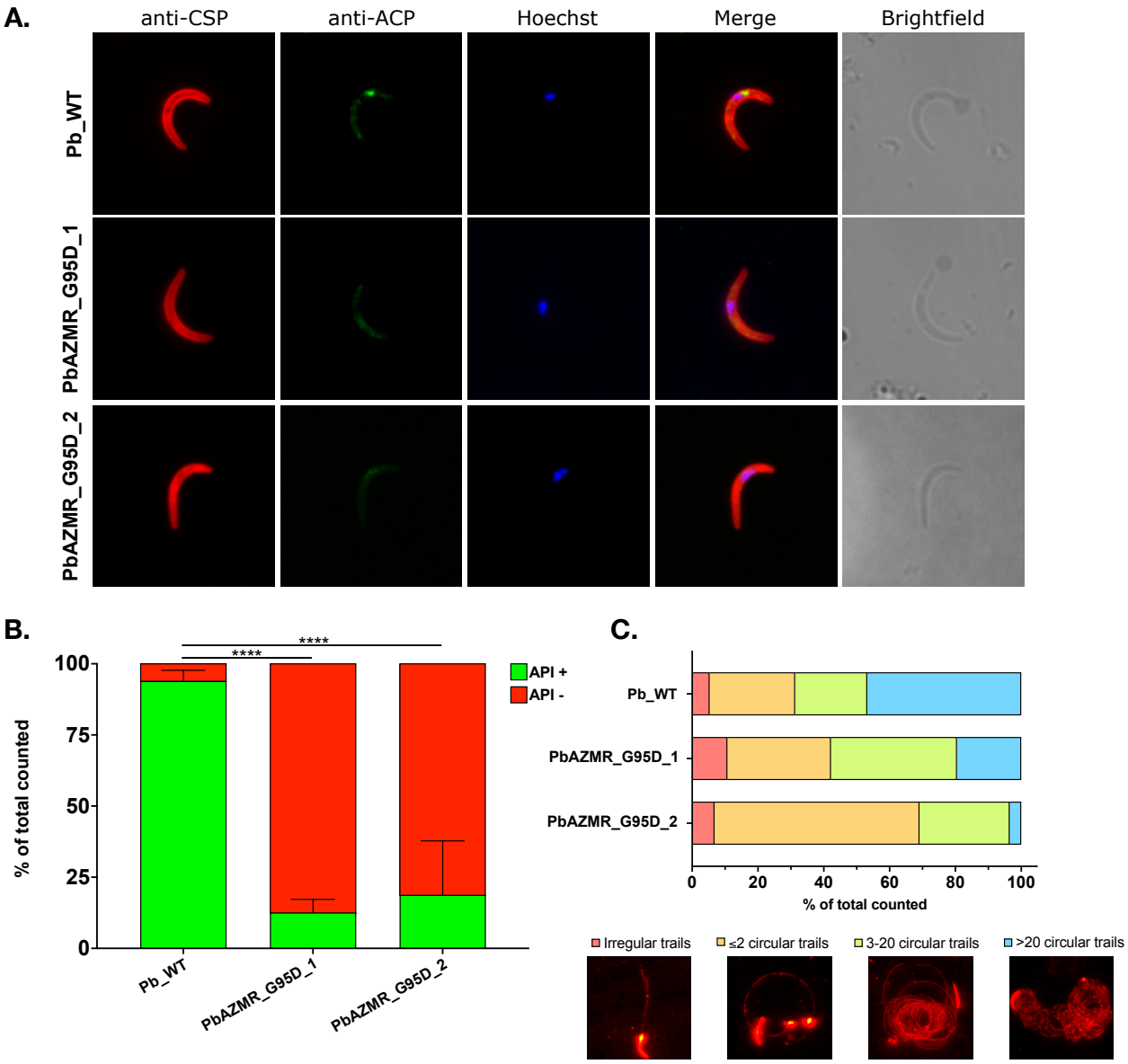

Figure 3. Immunofluorescence assay on PbAZMR_G95D_1, PbAZMR_G95D_2 and WT sporozoites reveals that azithromycin resistant sporozoites lose their apicoplast. A.) Sporozoites were stained with anti-circumsporozoite protein (CSP; red) to mark the outer surface of the sporozoite, anti-ACP (green) to mark the apicoplast, and Hoechst (blue) to mark the nucleus. WT sporozoites have a clear, punctate apicoplast (top panel), while azithromycin resistant sporozoites have diffuse apicoplast marker staining (bottom two panels). Images are representative of the calculated majority; B.) Quantification of apicoplast presence (API+, green) and absence (API-, red) in WT (n=2068), PbAZMR_G95D_1 (n=445), and PbAZMR_G95D_2 (n=855) sporozoites, where n=number of total sporozoites counted. A minimum of 110 individual sporozoites were counted for each parasite strain, for each of three independent mosquito infections. Green bars indicate the mean percentage apicoplast positive apicoplast, error bar represents +95% CI. Both azithromycin resistant strains produce sporozoites with significantly fewer intact apicoplasts than WT (P<0.0001, Fisher's exact test); C.) Quantification of sporozoite motility trails from PbAZMR_G95D_1 (n=159), PbAZMR_G95D_2 (169), and

1291 WT (n=175) sporozoites, from two independent mosquito infections. There was no significant
1292 difference in types of trails observed between each parasite line (chi-square test), and no
1293 correlation to apicoplast presence or absence (data not shown).
1294

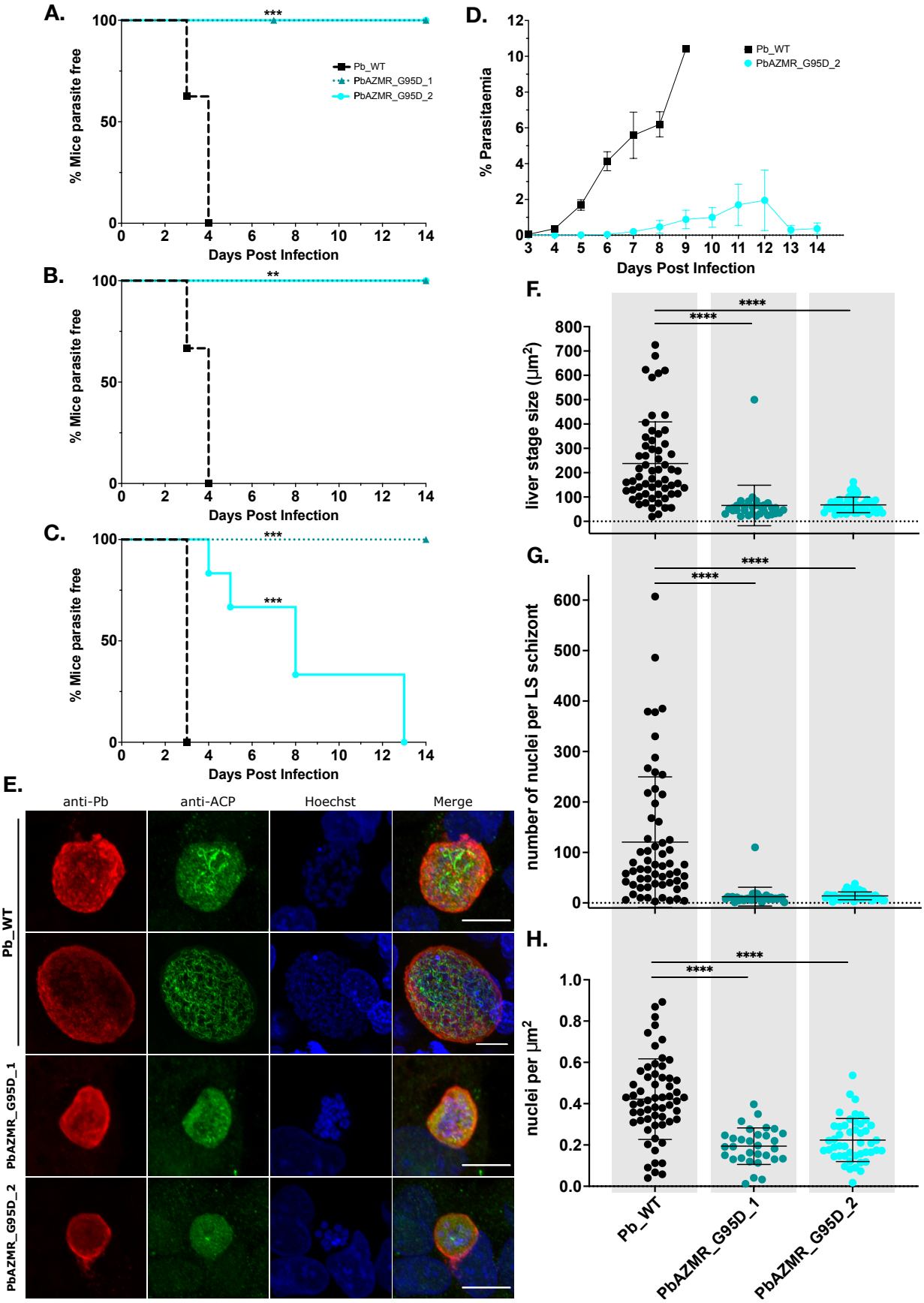
A.
% Mice parasite free
Days Post Infection
Pb_WT
PbAZMR_G95D_1
PbAZMR_G95D_2
***
B.
**
C.
***
D.
% Parasitaemia
E.
anti-Pb
anti-ACP
Hoechst
Merge
Pb_WT
PbAZMR_G95D_1
PbAZMR_G95D_2
F.
liver stage size (µm²)
****
G.
number of nuclei per LS schizont
H.
nuclei per µm²

1295

1296 **Figure 4.** Transmission of azithromycin resistant *P. berghei* parasites to a naïve host is severely
1297 impaired, and *in vitro* liver stage development appears stalled. A.) Kaplan-Meier curves of P0
1298 infections by biting. At least 15 infected mosquitoes were allowed to feed on naïve mice for at
1299 least 15 minutes and mice were monitored for 14 days by Giemsa smear (one mouse infected
1300 with PbAZMR_G95D_1 was only monitored until day 7, indicated by the initial triangle
1301 marker). Number of transmission attempts per strain were WT, n=8; PbAZMR_G95D_1, n=4;
1302 PbAZMR_G95D_2, n=4. Naïve mice infected with azithromycin strains by biting failed to
1303 establish an infection, and this was significantly different than WT (***P=0.0007, Mantel-Cox
1304 test) B.) Kaplan-Meier curves of P0 infections by $1x10^3$ IV of sporozoites. Mice were monitored
1305 for 14 days by Giemsa smear. Number of transmission attempts per strain were WT, n=6;
1306 PbAZMR_G95D_1, n=1; PbAZMR_G95D_2, n=4. Naïve mice infected with azithromycin
1307 strains by $1x10^3$ IV failed to establish an infection, and this was significantly different than WT
1308 (**P=0.01, Mantel-Cox test). C.) Kaplan-Meier curves of P0 infections by $1x10^4$ IV of
1309 sporozoites. Mice were monitored for 14 days by Giemsa smear. Number of transmission
1310 attempts per strain were WT, n=10; PbAZMR_G95D_1, n=5; PbAZMR_G95D_2, n=6. Only
1311 naïve mice infected with either WT or PbAZMR_G95D_2 by $1x10^4$ IV were able to establish an
1312 infection, but infection with PbAZMR_G95D_2 sporozoites showed delayed patency (mean 8.5
1313 days ± 3.8 days [SD]) and impaired growth. This was significantly different than WT
1314 (***P<0.0001, Mantel-Cox test). D.) Growth curve comparison of P0 infections established by
1315 WT and PbAZMR_G95D_2 by $1x10^4$ IV of sporozoites. Mice infected with PbAZMR_G95D_2
1316 sporozoites grow slowly, and would likely be outcompeted by fitter, WT parasites in a natural,
1317 mixed infection. Points shown indicate mean parasitaemia (±SEM), WT, n=9;
1318 PbAZMR_G95D_2, n=6, where 'n' represents the number of infected mice monitored for the
1319 period; E.) Immunofluorescence assay of liver cells infected with WT, PbAZMR_G95D_1 and
1320 PbAZMR_G95D_2 sporozoites in vitro and fixed at 48 hours post infection. The top two panels
1321 show HC-04 cells infected with WT sporozoites, the middle two panels show HC- 04 cells
1322 infected with PbAZMR_G95D_1 sporozoites and the bottom two panels show HC-04 cells
1323 infected with PbAZMR_G95D_2 sporozoites. Even the smaller WT liver stage schizonts show
1324 reticulated ACP staining (green) indicating normal apicoplast structure, while azithromycin
1325 resistant liver stage schizonts only show dispersed and cloudy ACP (apicoplast) staining. Nuclei
1326 (blue) in azithromycin resistant liver stage schizonts also appear clustered and donut-shaped,
1327 while WT liver stages show clear, individual nuclei. Red staining indicates anti-Pb, marking the
1328 outside of the liver stage parasite. All images are maximum projections and scale bars represent
1329 10 μm; F.) Quantification of parasite size (μm^2) at 48-hours post sporozoite inoculation of HC-04
1330 cells *in vitro* pooled from two independent experiments, with WT (n=60), PbAZMR_G95D_1
1331 (n=31), and PbAZMR_G95D_2 (n=47), where 'n'= number of individual liver stage schizonts
1332 measured. PbAZMR_G95D_1 and PbAZMR_G95D_2 liver stages are significantly smaller than
1333 WT (****P<0.0001, Ordinary one-way ANOVA with Dunnett's multiple comparisons test; bars
1334 represent the mean ±SD); G.) Pooled quantification of nuclei counts from the same liver stage
1335 schizonts quantified in F. PbAZMR_G95D_1 and PbAZMR_G95D_2 liver stages have
1336 significantly fewer nuclei than WT (****P<0.0001, Ordinary one-way ANOVA with Dunnett's
1337 multiple comparisons test; error bars represent the mean ±SD); H.) Nuclei counts, normalised to
1338 the size of each individual liver stage parasite described in F (number of nuclei per μm^2).
1339 PbAZMR_G95D_1 and PbAZMR_G95D_2 liver stages have significantly fewer nuclei than WT
1340 even when normalised to liver stage parasite size (****P<0.0001, Ordinary one-way ANOVA
1341 with Dunnett's multiple comparisons test; error bars represent the mean ±SD).

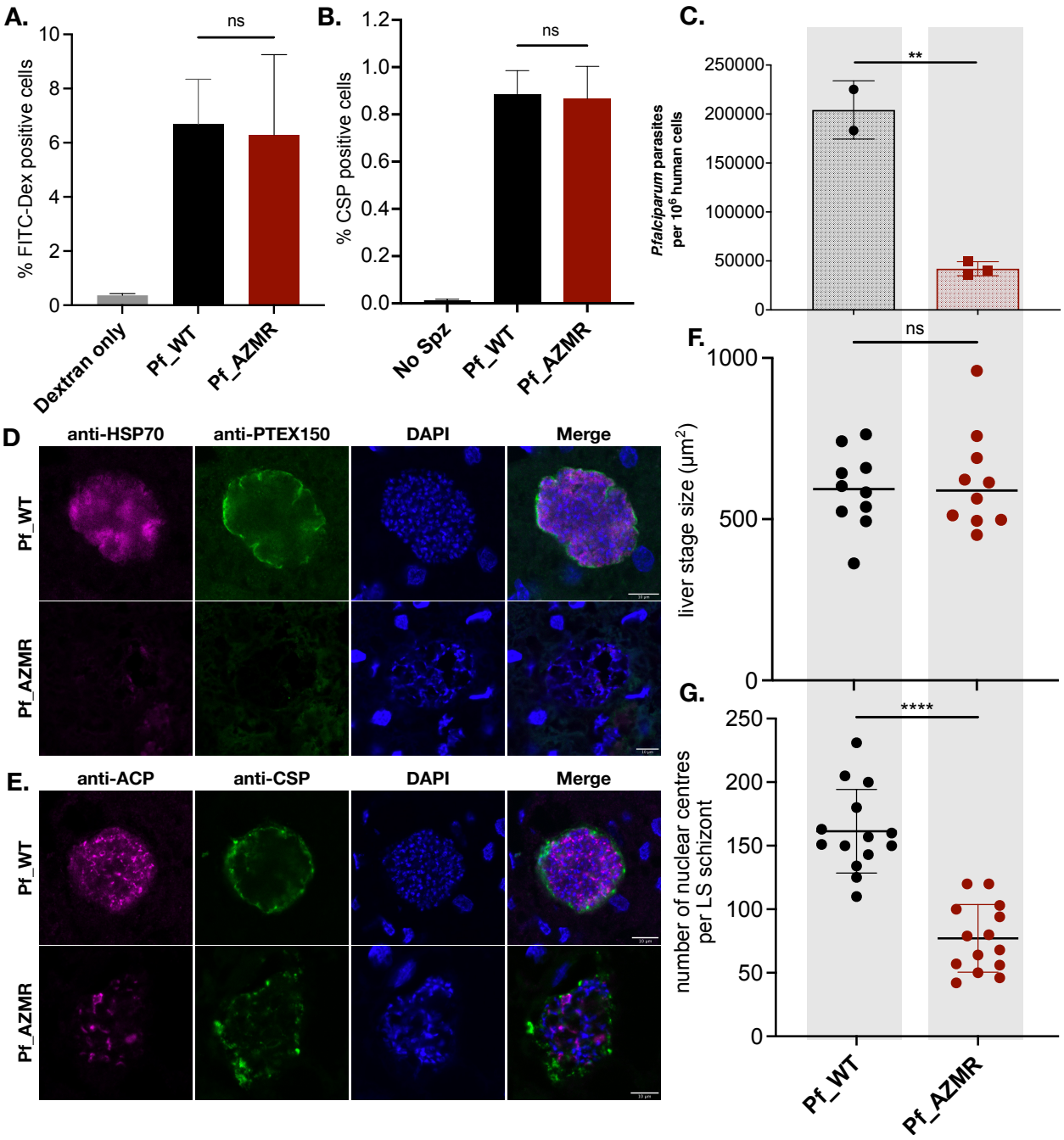

Figure 5. Liver stage development of *P. falciparum* azithromycin resistant parasites is impaired and parallels what we see with *P. berghei* azithromycin resistant strains. A.) HC-04 cell traversal by Pf_WT and Pf_AZMR sporozoites at multiplicity of infection (MOI) 0.3, measured by FITC-Dextran uptake and counted by FACS. Cells were fixed at 3 hours post inoculation and show no significant difference between Pf_WT and Pf_AZMR indicating normal sporozoite motility in azithromycin resistant parasites (ns = not significant, Paired t-test two-tailed P value); B.) HC-04 cell invasion by Pf_WT and Pf_AZMR sporozoites measured by FACS after incubation for 18-hours using CSP-positive antibody staining of fixed permeabilized cells. No significant difference was seen in invasion of HC-04 between Pf_WT and Pf_AZMR sporozoites (ns = not

significant, Paired t-test two-tailed P value); C.) Quantification of parasite liver load in humanised mice infected by i.v. injection of 8 x 10^5 Pf_WT sporozoites (n=2 mice) or Pf_AZMR sporozoites (n=3 mice) by qRT-PCR. Livers of infected humanised mice were harvested at day 5 post sporozoite i.v. and tissue homogenised for subsequent loads analysis and determination of the degree of chimerism. Pf_AZMR infected mice showed a significantly lower liver stage parasite load than mice infected with Pf_WT sporozoites (Unpaired t-test, two-tailed P value, P=0.0023, error bars represent mean ±SD); D.) Immunofluorescence assay of liver sections from livers of humanised mice infected with either Pf_WT or Pf_AZMR sporozoites. Liver stage schizonts were stained with anti-HSP70 (cytosolic marker) and anti-PTEX150 (parasitophorous vacuole marker) and DAPI DNA stain. Pf_AZMR liver stage schizonts show little to no staining with either anti-HSP70 or anti-PTEX150 and show aberrant nuclear staining, with individual nuclei unclear. Scale bar 10 μm; E.) Immunofluorescence assay of liver stage schizonts and stained with anti-ACP (apicoplast marker), anti-CSP (parasite marker) and DAPI DNA stain. Pf_AZMR livers stage schizonts show a loss of anti-ACP and anti-CSP stain compared to WT, and again show aberrant nuclear staining, with DAPI appearing to aggregate around holes. Scale bar 10 μm; F.) Quantification of liver stage schizont size (μm^2) from liver sections from livers of humanised mice infected with either Pf_WT or Pf_AZMR sporozoites. Sections from independent mice were selected and individual 'n' liver stage schizonts measured, Pf_WT (n=10), Pf_AZMR (n=10). No significant difference in liver stage schizont size was seen (ns = not significant, Unpaired t-test, two-tailed P value); G.) Quantification of nuclear centres counted from liver stage schizonts imaged in D and E. Pf_AZMR liver stage schizonts show significantly fewer nuclei than Pf_WT, indicating impaired liver stage development (Unpaired t-test, two-tailed P value, P<0.0001; error bars represent mean ±SD).

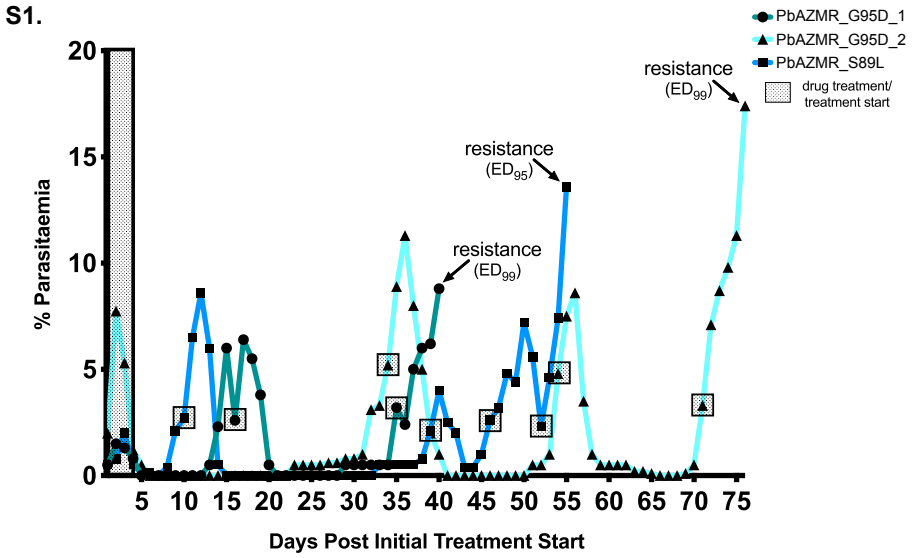

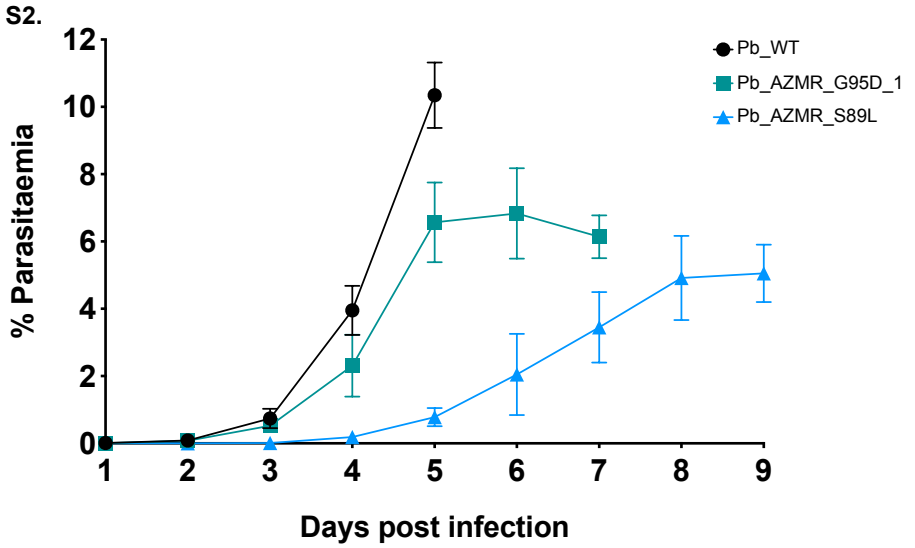

Figure S1. Generation of azithromycin resistant *P. berghei* parasites *in vivo*. PbAZMR_G95D_1 and PbAZMR_G95D_2 were both generated off a 70 mg/kg q.d. dosing regimen, and PbAZMR_S89L was generated off a 60 mg/kg q.d. dosing regimen. The initial four-day dose is represented by the shaded rectangle, and the start of each dose thereafter is indicated by a shaded box to avoid rectangle overlaps. Parasites were deemed resistant when they failed to reduce in parasitaemia on the third day post treatment start (with the exception of PbAZMR_S89L, which grew slowly so was monitored differently).

Figure S2. Blood stage growth of *P. berghei* azithromycin parasites is impaired compared to WT without drug pressure. Growth assay of PbAZMR_G95D_1 (n=3) and PbAZMR_S89L (n=3) compared to WT (n=3). Parasitaemia was monitored by Giemsa-stained thin blood smears. Dot points represent mean parasitaemia, and error bars indicate ±SD. Growth of both azithromycin resistant parasite lines is delayed compared to WT, and eventually fails to increase.